Coral microatoll partial mortality after multi-hour subaerial exposure: Implications for relative sea-level studies

Jennifer Quye-Sawyer*[1,2], Jing Ying Yeo[1,2], Wan Lin Neo[1,2], Fangyi Tan[1,2], Jun Yu Puah[1,2], Aron J. Meltzner[1,2]

[1]Earth Observatory of Singapore, Nanyang Technological University, Singapore
[2]Asian School of the Environment, Nanyang Technological University, Singapore

*Correspondence to: j.quye.sawyer@gmail.com

This is a preprint of a manuscript submitted for publication in *Scientific Reports*. Please note that the manuscript has yet to be accepted for publication, and subsequent versions of this manuscript may have slightly different content. If accepted, the final version of this manuscript will be available via the 'Peer-reviewed Publication DOI' link on this webpage.

Coral microatoll partial mortality after multi-hour subaerial exposure: Implications for relative sea-level studies

Jennifer Quye-Sawyer*[1,2], Jing Ying Yeo[1,2], Wan Lin Neo[1,2], Fangyi Tan[1,2], Jun Yu Puah[1,2], Aron J. Meltzner[1,2]

[1]Earth Observatory of Singapore, Nanyang Technological University, Singapore
[2]Asian School of the Environment, Nanyang Technological University, Singapore

*Corresponding author: J. Quye-Sawyer (j.quye.sawyer@gmail.com)

Abstract

Some intertidal corals, known as microatolls, have a distinct morphology that reflects changes in local relative sea level. While past observations have shown that the top surface of these corals may be killed by subaerial exposure, little is known about the exact oceanographic or environmental conditions that cause a coral to die down to a particular level. Here, we combine field surveys, tide-gauge data and analysis of microatoll morphology to investigate the survival limits of *Porites* spp. microatolls on Singapore's intertidal reefs. Unponded *Porites* spp. microatolls on the Pulau Biola reef reach a 'highest level of growth' between mean low water springs and mean low water neaps. Diedowns on the highest microatolls during 2023 and 2024 suggest the survival of these corals depends on the duration of subaerial exposure. By comparing the estimated highest level of survival after a diedown to water levels recorded at local tide gauges, we show that intertidal corals on the Biola reef and nearby Siloso Point reef can survive more than two hours of continuous subaerial exposure per day. However, *Porites* spp. corals may not have survived more than 3.5 hours of daily partial exposure without dying down.

1. Introduction

Relative sea-level (RSL) change is often driven by many processes operating over different spatial and temporal scales. For example, oceanographic phenomena such as the El Niño–Southern Oscillation (ENSO), glacial isostatic adjustment and dynamic topography affect RSL on a regional scale, while vertical land motion from tectonic deformation, sediment compaction and groundwater extraction usually have a more local effect[1,2]. Since all these processes can operate over multi-decadal timescales, or longer, environmental proxies are required to quantify changes in RSL beyond the short records provided by tide gauges and satellite altimetry data. Few proxies can resolve changes in water level over long enough time scales, and with sufficiently high precision, to identify the various drivers of RSL. Fortunately, one RSL proxy noted for its high temporal precision is the coral microatoll, which has been used to quantify seismic deformation[3–6] and Holocene relative sea-level trends[7,8] in low-latitude regions.

Microatolls are intertidal corals with a characteristic concentric-ring morphology on their dead upper surfaces (Figure 1). Each concentric ring forms due to a period of unconstrained upwards and outwards growth followed by a diedown that kills the living coral rim down to its highest level of survival (HLS) [9]. By assuming that changes in the HLS are driven by different magnitudes of subaerial exposure (emersion), microatolls are often considered to be 'natural tide gauges' with the ability to record water-level fluctuations to centimetre-scale precision over decades to centuries, depending on the lifespan of the coral colony[7,10–12].

Fossil microatolls can also be used to produce Holocene sea-level index points (SLIPs), a measure of paleo-RSL at a particular place and time. The vertical component of a SLIP can be calculated using the elevation difference between nearby fossil and living microatolls of the same species if we assume microatoll indicative meaning (proxy elevation relative to tidal datums) has not changed through time[6,12,13]. However, the proximal modern reef may not contain living microatolls of the same species as the fossils, which complicates the process of creating SLIPs. Studies at such sites have determined RSL using the theoretical relative elevations of different coral species[7,14] or employed a relationship between microatoll elevation and tidal datums that had been derived at another location[15–17]. The latter approach can be used even if there are no living microatolls nearby, but the association between microatoll elevation and tidal datums is poorly defined. For example, reef-flat microatolls at the microtidal Cocos (Keeling) Islands were found above mean low water springs (MLWS)[18], and microatolls at the microtidal Cook Islands lie in a narrow elevation range between MLWS and mean low water neaps (MLWN)[19], yet the highest level of growth (HLG) surveyed was below MLWS at the mesotidal Siloso Point reef, Singapore[8].

Apparent regional differences in the indicative meaning may arise because tides alone are not fully reflective of exposure duration: climatic sea-level anomalies (e.g. ENSO), storm surges, and other processes also contribute to subaerial exposure of the reef[11,20,21]. In general, experiments and observations suggest that corals die once a threshold exposure time is exceeded[22–27]. Corals of many species can survive several hours out of water, possibly because polyp retraction and the production of mucus limit desiccation when initially exposed to the air[29,30], yet survival thresholds are poorly quantified for the *Porites* spp. corals commonly used for microatoll-based sea-level reconstructions. Therefore, to better understand the precision and limits of microatolls as sea-level proxies, we require more constraints on the variability of microatoll growth within and between reef environments.

In this study, we use multi-year observations of microatoll emersion, bleaching and partial mortality to quantify the link between subaerial exposure and diedown occurrence. First, we describe the timing and extent of *Porites* spp. microatoll partial mortality at the Pulau Biola (BIOL) reef, Singapore, in 2023 and 2024. We then combine the morphology of Pulau Biola microatolls and local tide-gauge data to quantify the possible exposure duration threshold for coral mortality. We supplement our study of exposure duration with additional analysis of previously surveyed microatolls from the nearby Siloso Point (SILO) reef.

2. Study area

Singapore's coral reefs exist within a highly urbanized environment, where commercial shipping, land reclamation and dredging have resulted in a loss of reef area and created high turbidity in shallow water[31,32]. Nonetheless, coral cover on Singapore's remaining subtidal reefs has a mean value of approximately 24%[33], and the intertidal zone hosts many species of hard corals including the microatoll-forming *Porites lobata* and *Porites lutea*[34–36]. Pulau Biola (Violin Island), 12.5 km south of mainland Singapore, is an uninhabited islet and fringing reef with a total area of 0.08 km^2 (Figure 2). The reef substrate at Pulau Biola consists of the steeply dipping bedrock of the Tanjong Rimau Formation partially covered by sand, gravel and fossil coral rubble[37,38]. While much of Singapore's coastline been modified by land reclamation or construction of sea walls, the Biola reef and its rocky shoreline have not been subject to apparent alteration. Most of the lower reef flat to the north and west of the island freely drains to the open sea. However, on the upper foreshore and reef flat to the east of the island, exposed bedrock and gravel bars form local topographic depressions that retain seawater at low tide (Supplementary Figure S5).

The Siloso Point intertidal reef, Sentosa Island, is part of an approximately 500 m long east–west trending shoreline. Most living microatolls are found on the reef crest, seaward of a sandy and muddy beach protected by a rock revetment[8]. Land reclamation occurred to the east of the reef in the mid-2000s but the natural rocky shoreline and cliffs remain to the west[39,40]. Holocene fossil corals are found alongside the living microatolls at the Siloso Point study site, suggesting that the reef itself is unaltered[8].

Singapore lies at the transition between the diurnal tidal regime of the South China Sea and the semidiurnal tidal regime of the Indian Ocean, with mixed semidiurnal water level oscillations and diurnal tidal current oscillations in the Singapore Strait[41,42]. Low spring tides occur from pre-dawn to mid-morning between April and September and from late afternoon onwards between October and March. Both the 4.4-year perigee cycle and 18.61-year nodal cycle are present in the tide gauge records of Singapore and southern Peninsular Malaysia[43,44]. In addition, monsoon winds produce intra-annual sea-level anomalies of up to ±20 cm[46]. The largest East Asian-Western Pacific monsoonal influence occurs in the eastern Singapore Strait where the wet northeast monsoon produces positive sea level anomalies in October to March, and the drier southwest monsoon creates negative sea-level anomalies in April to September. The South Asian-Indian monsoon has increasing influence towards the west of the Singapore Strait, where additional negative sea-level anomalies occur in March and July/August[45,46]. ENSO and the Indian Ocean Dipole (IOD) also affect sea level height by up to 10 cm[46]. The minimum annual near-surface ocean temperatures in the Singapore Straits (≈27°C) occur during January and February. Annual near-surface ocean temperatures peak at ≈31°C, usually in June[47].

The Raffles Lighthouse tide gauge on Pulau Satumu is approximately 400 m south-southeast of Pulau Biola (Figure 2c). Water levels are recorded by the tide gauge in 6-minute increments and reported to centimetre precision. The Raffles Lighthouse tide-gauge data available for this study span from October 1996 to December 2021.

The Siloso Point tide-gauge record (Figure 2d) is produced from overlapping deployments of ONSET HOBO U20-001-04-Ti pressure-sensor tide gauges, calibrated using field measurements of water level. The Siloso Point tide-gauge data used in this study were collected between 2021 and 2024, and a detailed description of the tide-gauge data processing can be found in Supplementary Text S1. The Siloso Point microatolls analysed in this study lie less than 300 m from the tide gauge (Figure 2d).

3. Methods

3.1. Monitoring and surveying intertidal corals

Porites spp. intertidal coral colonies of the Pulau Biola reef were monitored between April 2022 and August 2024. Fieldwork at Pulau Biola was undertaken on one or two days per month during spring low tides of the southwest monsoon (April to September) when the intertidal reef was accessible on foot. At Siloso Point, we repeatedly observed several *Porites* spp. corals (SILO-L1, -L2, -L4 and, from 2021, -L5) in July and August 2020 and from February to October 2021. During each field visit, we visually examined the corals for evidence of recent diedowns, bleaching and signs of disease. We characterise bleaching as whitening of the coral surface and diedowns as areas of partial mortality that extend down the outer rim from the upper part of the coral colony.

We define living microatolls as corals with evidence of past diedowns caused by subaerial exposure. Specifically, we searched for concentric rings of dead coral on the upper surface of the colony and/or a living outer rim at a consistent elevation around the coral perimeter. We surveyed the unponded HLG and, if applicable, post-diedown HLS of *Porites* spp. microatolls of the Biola reef during our field visits of 2023. We measured the HLG of the Siloso Point microatolls in 2020 and 2021. Surveys were performed using a total station, and measurements obtained on different days were converted to the same relative height datum using local temporary benchmarks established in bedrock, concrete or fossil corals adjacent to the reefs.

To investigate how open-water sea-level changes are reflected in microatoll surface morphology, we noted whether the microatolls were situated in areas that were freely draining at low tide or if they were found in ponded water. We identified unponded *Porites* spp. microatolls as those that were either (a) fully exposed during at least one field visit, or (b) situated in water connected to the open ocean, with no seaward reef topography that could cause ponding, and where water levels changed according to the falling or rising tide.

We did not survey overgrowth because these out-of-sequence rings may survive at a slightly higher elevation than the coeval outer living rim (e.g. Figures 5 and 14 of ref.[48]; Figure S13a of ref.[3]), possibly due to localised water retention on the microatoll's upper surface at low tide (Figure 1b).

To analyze microatoll ring morphology, we created 3D models of the microatolls using the inbuilt iPhone 13 Pro LiDAR scanner and Scaniverse application (https://scaniverse.com). We conducted the LiDAR scans in 2023. The corals were scanned when fully exposed at low tide after we removed sediment from the dead upper microatoll surface to reveal the ring structure. We used CloudCompare (https://cloudcompare.org) to interpolate the LiDAR point cloud and create a plan-view digital surface model (DSM) of the microatoll's morphology[8,49], from which elevation profiles were extracted using the Generic Mapping Tools (GMT)[50]. Further details are given in the Supplementary Information.

3.2 Quantifying coral exposure thresholds

During the falling tide, water levels drop, and the reef becomes progressively subaerially exposed. First, the upper surfaces of the highest microatolls emerge from the water. More coral is progressively emersed until the lowest tide of the day, though, for ponded microatolls, maximum exposure magnitude is driven by the height of the sill surrounding the pond. Subsequently, the tide rises and the reef is flooded until all of the microatolls are submerged. The lowest microatolls are emersed for a shorter duration than the highest microatolls, and the upper tips of the microatoll's living outer rim are exposed for longer than the rest of the microatoll's living outer rim.

We surveyed the Raffles Lighthouse tide gauge benchmark relative to our temporary benchmarks on Pulau Biola and used the tide-gauge record to calculate the lowest intertidal elevation exposed above the water for a continuous 1-, 2-, 3- or 3.5-hour interval per day during 2021. We compared these elevations to microatoll HLS to estimate the daily duration of exposure for the Biola reef microatolls. For the corals at Siloso Point, we calculated the lowest elevation exposed per day using the Siloso Point tide-gauge record.

For both tide gauges, we also used the Unified Tidal Analysis and Prediction (UTide) models[51] to estimate MLWS and MLWN relative to lowest astronomical tide (LAT) for the 18.61-year period between 2004 and 2023. We build on earlier work at Siloso Point[8] by re-calculating tidal datums using a longer water-level time series obtained from January 2021 to June 2024.

4. Results

4.1. Microatoll elevations relative to tidal datums

Mean 2023 HLG for the Biola reef unponded microatolls was 44.3 cm (± 2.7 cm, 1 s.d. of repeat measurements of the tide-gauge benchmark) above admiralty chart datum (ACD), equal to 11 cm above MLWS at the Raffles Lighthouse tide gauge (Figure 3). The 2023 HLG for these corals is below the midpoint of MLWS and MLWN, which has been assumed to be the upper limit of unponded microatoll growth[52]. The HLG of the unponded corals at Pulau Biola was, as expected, lower than the HLG of ponded *Porites* microatolls. The average elevation of the highest ponded microatolls' living rims (and dead microatoll centre) is 79 cm above ACD, over 20 cm above the highest unponded surveyed microatoll (Figure 3).

The weighted mean HLG of all living *Porites* microatolls at Siloso Point is 1.42 ± 0.04 m below Singapore Height Datum (SHD; uncertainty is 2 standard errors of the weighted mean of 24 microatolls)[8]. MLWS at the Siloso Point site is 1.34 m below SHD based upon the Siloso tide-gauge data from January 2021 to June 2024. Therefore, the weighted mean of the 2021 HLG of the Siloso Point reef microatolls was below MLWS.

4.2. Microatoll diedowns at Pulau Biola in 2023 and 2024

BIOL-L13 (the highest-elevation unponded coral surveyed on the intertidal reef flat) had a raised outer rim that was bleached but apparently alive in May 2023 (Figure 4a). However, by August 2023, the top of the outer rim was dead and covered by sediment (Figure 4b). Therefore, we infer that BIOL-L13 died down at some point between May and August 2023. During our surveys of July and August 2023, we also observed apparent recent diedowns on other *Porites* spp. microatolls (BIOL-L13a, BIOL-L38 and BIOL-L56), though we do not have close-up photographs of these corals taken prior to the partial mortality event. BIOL-L13a had a diedown of similar magnitude to that seen on BIOL-L13 (Figure 4e) but BIOL-L56 and BIOL-L38 had patches of recently dead coral only on the tops of their outer rings (Figure 4f-h). The living rims of BIOL-L13a, BIOL-L56 and BIOL-L38 had not grown outwards beyond the adjacent dead coral by more than a few millimeters in August 2023. Since reported growth rates of Indo-Pacific *Porites* corals span ≈0.5 to 3 cm yr^{-1} [53–56], we infer that the partial mortality of BIOL-L13a, -L56, -L38 probably occurred within the preceding weeks or months and is likely coeval with the diedown on BIOL-L13.

We measured BIOL-L13's pre-diedown HLG and post-diedown HLS on 15 swath profiles extracted from the DSM (Figure 5). The DSM was created from a LiDAR scan taken on 5th August 2023, shortly after the mid-2023 diedown. The difference between BIOL-L13's pre-diedown HLG and post-diedown HLS (on 5th August) was 1.4 ± 0.7 cm (1σ) and was largest between the north and west faces of the microatoll, where a maximum difference of 2.6 cm was measured (Figure 5c). On 5th August 2023, we also used the total station to survey eight paired measurements of HLG and HLS at the approximate positions of the N, NE, E, SE, S, SW, W and NW swath profiles. The HLG–HLS difference from the field survey is 1.2 ± 0.3 cm (1σ).

We did not observe any diedowns between August 2023 and May 2024. The upper surfaces of BIOL-L13 and BIOL-L13a's outer rims were dead in August 2024 (Figure 4c,d; Supplementary figure S5), so we infer that there was an additional, smaller diedown on BIOL-L13 and -L13a between May and August 2024.

While BIOL-L13 was bleached in the month(s) before the diedowns (April 2023 and May 2024), bleaching was also present on many other *Porites* spp. corals that were exposed at low tide, including those that survived without partial mortality (Figure 4i,j, and Supplementary Figure S5). Therefore, bleaching does not necessarily presage diedowns on the Biola reef microatolls.

4.3. Exposure duration and microatoll survival

4.3.1 Pulau Biola microatolls

We combine water levels and coral elevations to determine the threshold exposure duration for diedowns. From the Pulau Biola reef, we use BIOL-L14, BIOL-L3 and BIOL-L13 as these corals have been continuously monitored since 2022 and thus the best constrained growth history of any unponded microatolls at this site.

BIOL-L14 has several concentric rings on its dead upper surface, which suggests this coral's morphology has developed in response to the process that forms microatolls (Figure 4i). However, despite being fully exposed during several field visits, this coral did not have a diedown between June 2022 (when first photographed) and August 2023 (when the HLG was surveyed, and the coral was scanned using LiDAR). In June 2022, the microatoll's living outer ring was approximately one centimetre thick, so, given a possible growth rate between ≈0.5 and 3 cm yr^{-1}, BIOL-L14's most recent diedown may have occurred during 2021.

While HLS can be precisely measured from radial slabs of coral using annual density or luminescence banding, we did not have permission to sample live coral for this study. Therefore, we estimate the post-diedown HLS using non-destructive LiDAR scans. To estimate the HLS after this most-recent diedown, we measured ring thickness from 14 swath profiles extracted from the LiDAR-derived DSM at angles perpendicular to the microatoll perimeter (Supplementary Figure S11). We assumed ring boundaries beneath the microatoll surface are parallel to the outer living rim and that vertical and lateral growth rates are equal. Mean ring thickness across all profiles is 2.5 ± 0.64 cm, and HLG in August 2023 was 41.0 ± 1.53 cm above ACD. Therefore, we estimate the HLS after BIOL-L14's most recent diedown to be 38.5 ± 1.66 cm above ACD.

We assume water levels recorded at the nearby Raffles Lighthouse tide gauge (Figure 2c) are representative of the tides and sea-level anomalies on the Biola reef. Under this assumption, BIOL-L14 would have been fully emersed for at least an hour on 19 days in 2021 when the recorded water level was lower than the base of the coral for a continuous 1-hour period (Figure 6c). While we did not monitor the Biola reef microatolls in 2021 (the most recent year of our tide-gauge data), full subaerial exposure of intertidal corals was recorded on Singapore's other reefs between April and August 2021[57,58], so emersion of the Biola reef microatolls during these spring low tides seems reasonable based upon observations elsewhere in the region. The tide-gauge data also suggests BIOL-L14 would have been fully exposed for at least two continuous hours during four days between May and July when water levels were lower than the reef substrate surrounding the coral (Figure 6d). Since at least part of BIOL-L14 must have remained alive throughout 2021, we therefore infer that BIOL-L14 can survive more than two hours out of water.

BIOL-L14 would not have been fully subaerially exposed for three or more consecutive hours per day during 2021, but this coral would have been partially exposed for a three-hour duration on several occasions. The estimated HLS of BIOL-L14's most recent diedown coincides with the lowest elevation exposed for three hours per day between 28th and 30th May 2021 (Figure 6e). If the most recent diedown happened in 2021, at least three hours of continuous subaerial exposure above the estimated HLS (≈39 cm ACD) may have been sufficient to kill the part of the coral's outer rim that was exposed above the water for this time. Coral polyps below ≈39 cm ACD must have survived throughout 2022, and coral polyps in this lower region of BIOL-L14's outer perimeter would have been exposed for less than three hours per day in 2022.

BIOL-L3, another microatoll first observed in 2022 and with no diedowns from April 2022 to August 2023, would also have been partially exposed for three hours down to the elevation, within error, of its most-recent HLS in June 2021 (Supplementary Figures S12, S16).

BIOL-L13's most recent pre-2023 diedown (based upon ring thickness estimated from the DSM; Supplementary Figure S13) would have been approximately 10 cm higher than that of BIOL-L14 and BIOL-L3 (Figure 6; Supplementary Figure S12). As such, BIOL-L13 would have been both fully and partially exposed more frequently and for a longer maximum daily exposure duration than BIOL-L14 or BIOL-L3. In 2021, BIOL-L13 would have been partially exposed for approximately 3.5 hours down to the elevation of the pre-2023 diedown HLS according to the Raffles Lighthouse tide-gauge data (Figure 6f).

4.3.2 Siloso Point microatolls

Microatolls on the Siloso Point reef are inferred to have died down in early–mid 2020, but no diedowns were observed between July 2020 and the start of 2021[8]. Bleaching was observed on the *Porites* microatolls at Siloso Point in May 2021, and we noticed partial mortality of some Siloso Point microatolls in mid-2021 (Supplementary Figure S6).

Of the corals surveyed in 2020 and 2021, SILO-L1 and SILO-L2 had the highest HLG prior to the 2021 diedown. The top of SILO-L1's outer ring died between 29th May and 13th June 2021 (Supplementary Figure S6). A similar diedown of centimetre-scale magnitude was observed on SILO-L2 when it was photographed on 27th June 2021. SILO-L4, a microatoll with lower-elevation pre-diedown HLG, also had a centimetre-magnitude diedown between 29th May and 28th June. Assuming coeval partial mortality on SILO-L1, -L2 and -L4, these field observations therefore constrain the diedown timing to the period between 29th May and 13th June. However, SILO-L5, which was first photographed on 27th June 2021, showed no indication of a diedown within the preceding months (Supplementary Figure S6). None of SILO-L1, -L2, -L4 or -L5 had signs of new partial mortality between June and October 2021 (Supplementary Figure S7).

We surmise that the upper parts of SILO-L1, -L2 and -L4 were partially exposed for a sufficient time duration to cause mortality of the upper parts of the coral colonies, but the small magnitude of the 2021 diedown on SILO-L1, -L2 and -L4 suggests the threshold exposure duration was exceeded only at the tips of their living rims (within a centimetre of their HLG in May 2021). The pre-2021 diedown HLG of SILO-L1 and SILO-L2 was surveyed on 1st May 2021 and 24th July 2020, respectively (Figure 7). The pre-diedown HLG of SILO-L4 was surveyed on 1st April 2021 (Figure 7). We extrapolated the surveyed HLG values until the end of May 2021 by assuming a vertical growth rate between 0.5 and 3 cm yr^{-1}. From the extrapolated HLG and the Siloso tide-gauge record, we infer that SILO-L1 and SILO-L2 were exposed for two continuous hours per day on six occasions in March and April 2021 (Figure 7a), though no diedowns were observed at these times. The upper tips of SILO-L1's and SILO-L2's outer living rims were first exposed for approximately three consecutive hours during the spring low tides of 28th to 30th May 2021 (Figure 7b). Similarly, SILO-L4 was first exposed for more than two hours on 28th May (Figure 7a). Therefore, the vertical growth of these corals appears to have been limited by the relatively long exposure duration at the end of May 2021. Since SILO-L1 and SILO-L2 had the highest pre-diedown HLG of any surveyed corals on the Siloso Point reef, we suggest three hours of exposure per day may be the upper limit of *Porites* microatoll survival at this location.

Prior to the 2021 diedown, the highest HLG of SILO-L5 was similar to that on SILO-L4, both of which were lower than the highest HLG on SILO-L1 and SILO-L2. No part of SILO-L4 or SILO-L5's living outer ring was subaerially exposed for three or more hours in 2021 (Figure 7b), but at least part of SILO-L5's outer ring was exposed for two or more hours on ten occasions between May and July. We infer that SILO-L5 was not exposed for long enough for a diedown to occur, even though the maximum HLG of SILO-L5 and SILO-L4 was similar at the end of May 2021.

5. Discussion

At Pulau Biola and Siloso Point, we observed microatolls surviving short periods of emersion without partial mortality, and diedowns occurring only on the parts of the microatolls exposed for the longest duration, which supports the hypothesis of a threshold exposure time before coral death occurs.

The observed diedown timings (May–August at Pulau Biola and May–June at Siloso Point) coincide with the relatively low tides of the 18.61-year nodal cycle and negative sea-level anomalies of the southwest monsoon[43-46], which suggests partial mortality was caused by subaerial exposure of the microatolls. However, these extreme low water levels were not sufficient to cause partial mortality of all intertidal corals. Only the highest corals had a diedown during the observation period at Pulau Biola, and the post-diedown HLS on BIOL-L13 was several centimetres higher than the HLG of surveyed corals that did not die down in 2023 (Figure 3b). For the microatolls at Pulau Biola that did not die down in 2023, the 2023 HLG was lower than the crests of the older rings (e.g. Figure 4i,j), suggesting that these corals may have slower growth rates and did not grow up to the level that would be limited by subaerial exposure. Faster growing microatolls may therefore be advantageous in RSL studies. The observed diedown timing also implies that monsoon strength, as well as the amplitude of the multi-annual tidal cycles, may influence the likelihood of diedowns on Singapore's corals in any given year.

Although the observed diedown timings also coincide with the annual maximum near-surface water temperatures[47] in the Singapore Strait, we suggest that thermal stress when the microatolls were submerged cannot exclusively explain the occurrence of diedowns. This is because we have no evidence for diedowns occurring at the end of 2023, when water temperatures were similar to June of that year due a strong El Niño[47].

While our analysis of the 2021 tide-gauge data suggests a minimum threshold daily emersion time of >2 hours may have caused diedowns of the Biola and Siloso Point reef microatolls, we cannot ascertain the precise relationship between diedown timing and total exposure over a spring low tide cycle due to our limited monitoring during field visits. It is possible that microatoll survival depends on cumulative exposure over longer (daily and monthly) periods, similar to observations of tissue loss on *Pocillopora* corals only occurring after multiple exposure events[30].

Paleo sea-level studies may also aim to create a longer, continuous record of RSL by combining HLG records from microatolls of overlapping ages. However, as observed at the Biola site in 2023 and the Siloso Point site in 2021, an extreme low water level episode may only (partially) kill higher corals on the intertidal reef, producing coeval fossil microatolls with different ring morphologies. The post-diedown HLS may also vary between those coral colonies that experienced mortality. The post-diedown HLS of BIOL-L13 and BIOL-L13a was higher than that of other corals that simultaneously died down at Pulau Biola in 2023, and the relatively high HLS elevation of BIOL-L13's previous diedown (the diedown prior to 2023; Figure 6) suggests this coral is more tolerant of exposure than others at the site. Corals could only be identified at the genus level for this study, and it is possible that tolerance to exposure may differ between *Porites* species, or even between more resilient genotypes of the same species[59]. Therefore, we suggest that ring morphology, coral elevation and natural biological variability always be considered when interpreting microatoll fossils at a site. Simulations of microatoll growth[60,61] could be a useful method to constrain RSL histories from multiple coeval but morphologically different microatolls.

While the development of microatoll morphology is probably driven by exposure duration, the indicative meaning of a paleo sea-level proxy is conventionally described relative to tidal datums[52,62]. The HLG of all surveyed unponded *Porites* microatolls on the Biola reef was above MLWS, yet no equivalent corals at the Siloso Point site had HLG significantly above this tidal datum, which implies a different indicative meaning for two reef sites only ~10 km apart. The microatolls on the Biola reef were surveyed in 2023, several years after the surveys at Siloso Point, and the Siloso Point microatolls may have continued to grow vertically during late 2021 and 2022. Nonetheless, the slow (up to 3 cm yr^{-1}) growth rate for *Porites* spp. constrains the maximum HLG in any given year, so some Siloso Point microatolls (those lower than SILO-L5), could not have grown higher than MLWS by mid-2023. We suggest that the apparent difference in the indicative meaning between the two sites may arise from the high spatial variability in nontidal (e.g. monsoon-related) sea-level anomalies across the Singapore Strait[46] (Supplementary Figure S4), or that there is a greater natural variability in *Porites* HLG than can be captured by surveys at a single reef. In general, if the probability of a diedown depends on exposure duration, RSL studies using microatolls should consider all drivers of sea-level variability, not just estimated tidal datums, to form an indicative range for SLIPs.

The apparent exposure duration threshold for microatolls diedowns has implications for RSL studies. Where living microatolls are not found adjacent to a fossil microatoll site, tide-gauge data could be used to find the elevation that would be exposed for the threshold exposure time for coral mortality. This theoretical elevation for mortality could then be used to check the validity of the assumed indicative meaning, or RSL could even be quantified directly using the fossil coral elevations and the tide-gauge data.

Environmental conditions during emergence, such as temperature, precipitation and wave splash, may also influence coral survival at both the Biola and Siloso Point reefs. Both observational and experimental data suggest that intertidal corals are more tolerant of exposure under conditions of low solar irradiance[24,63,64]. Since the reefs in this study are situated at low latitudes (1° N of the equator), seasonal differences in temperature and irradiance are minimal[65]. Nonetheless, exposure of the Biola and Siloso Point intertidal reefs often begins before sunrise or ends after sunset (Figure 6; Figure 7), and it is possible that exposure spanning dawn or dusk increases the time that these corals can survive out of water compared to *Porites* microatolls in a different tidal regime.

Some coral reefs appear to acclimatize to elevated temperatures[66,67], which suggests that *Porites* microatolls could become more tolerant of environmental stressors over time. In addition, corals may inherit a tolerance for more extreme conditions, such as high temperature[68]. Therefore, it is possible that microatoll fields may adapt to changing environments across generations, resulting in different elevations relative to tidal datums over time. Greater mortality has also been observed on larger coral colonies than expected based upon their relative subaerial exposure alone[69], suggesting corals may be more susceptible to emersion as they age. At the Biola reef we did not find a relationship between microatoll size (a proxy for coral age) and diedown occurrence, though we acknowledge that most microatolls in this study are probably less than 50 years old based upon their diameters and assumed growth rate (BIOL-L14, with an average radius of ≈45 cm in 2023, was the largest surveyed microatoll). Finally, we do not know whether anthropogenic disturbance of coral reefs may have changed the survival limits of microatolls, which is particularly important for studies that quantify past sea level using the relative elevations of fossil microatolls and their living counterparts.

6. Conclusions

To accurately use coral microatolls as RSL proxies, their relationship to tidal datums and subaerial exposure conditions needs to be quantitatively understood. Information on the exposure duration that cause a diedown has been lacking, in part because many intertidal reefs are poorly suited for long-term monitoring and tide-gauge data are difficult to obtain. Our findings at Pulau Biola provide further evidence that coral microatolls inhabit a narrow elevation range in the lower intertidal zone, reinforcing the suitability of fossil microatolls for paleo-sea-level studies. The HLG of unponded

Porites microatolls of the Biola reef in 2023 was above MLWS, while the HLG of microatolls at the Siloso Point reef was below MLWS, with the two sites only ~10 km apart. However, observations at both sites reveal that *Porites* microatolls on Singapore's reefs can tolerate more than two hours of exposure per day before dying down, and no corals are inferred to have survived more than approximately 3.5 hours of exposure in 2021.

Acknowledgements

Primary funding for this work came from the National Research Foundation (NRF) Singapore under its Singapore NRF Fellowship scheme (Award NRF-NRFF11-2019-0008 to A.J.M.). This research was also supported by the Singapore Ministry of Education (MOE) Academic Research Fund (Award MOE2019-T3-1-004 to A.J.M.). Fieldwork was conducted under Singapore National Parks permit NP/RP20-122. We are grateful to the Maritime and Port Authority of Singapore (MPA) for the Raffles Lighthouse tide-gauge data and for permitting access to Pulau Satumu. We also thank the Singapore Ministry of Defence for allowing fieldwork at Pulau Biola. We acknowledge the support of the Sentosa Development Corporation team, particularly G. Lee, L. Tan, and the Sentosa environmental management team for fieldwork at Siloso Point. Rohan Gautam, Valerie Sng Hui Xuan and Joylynn Goh Xin En are thanked for fieldwork assistance and helpful discussions. This is Earth Observatory of Singapore contribution 653.

Author contributions

J.Q.S. conceptualised the study, devised the methodology, produced the digital surface models and led all data analysis. J.Q.S., J.Y.Y., W.L.N., F.T. and A.J.M. conducted the fieldwork. J.Y.Y., W.L.N., F.T. and J.Q.S. processed the Siloso Point tide-gauge data. J.Y.P. processed the Raffles Lighthouse tide-gauge data and calculated tidal datums. A.J.M. provided the funding and supervised the project. J.Q.S. wrote the manuscript with input from all authors.

Data availability

The Siloso Point tide-gauge data and LiDAR scan point clouds relevant to this study are available in the Zenodo repository at https://doi.org/10.5281/zenodo.15422742. The Siloso Point coral and benchmark survey data are available in the DR-NTU data repository at https://doi.org/10.21979/N9/BRBZQC. The Raffles Lighthouse tide-gauge data are property of MPA. All other data generated and analysed during this study are included in this published article (and its Supplementary Information files).

Additional information

The authors declare that they have no competing interests.

References

[1] Rovere, A., Paolo, S. & Vacchi, M. Eustatic and relative sea level changes. *Curr. Clim. Change Rep.* **2**, 221–231 (2016).

[2] Yokoyama, Y. & Purcell, A. On the geophysical processes impacting palaeo-sea-level observations. *Geosci. Lett.* **8**, 13 (2021).

[3] Meltzner, A. J. *et al.* Coral evidence for earthquake recurrence and an AD 1390–1455 cluster at the south end of the 2004 Aceh–Andaman rupture. *J. Geophys. Res. Solid Earth* **115**, B10 (2010).

[4] Shyu, B. H. *et al.* Upper-plate splay fault earthquakes along the Arakan subduction belt recorded by uplifted coral microatolls on northern Ramree Island, western Myanmar (Burma). *Earth Planet. Sci. Lett.* **484**, 241–252 (2018).

[5] Philibosian, B. E. *et al.* 20th-century strain accumulation on the Lesser Antilles megathrust based on coral microatolls. *Earth Planet. Sci. Lett.* **579**, 117343 (2022).

[6] Taylor, F. W., Frohlich, C., Lecolle, J. & Strecker, M. Analysis of partially emerged corals and reef terraces in the central Vanuatu arc: Comparison of contemporary coseismic and nonseismic with Quaternary vertical movements. *J. Geophys. Res.* 92, 4905–4933 (1987).

[7] Yu, K.-F., Zhao, J.-X., Done, T. & Chen, T.-G. Microatoll record for large century-scale sea-level fluctuations in the mid-Holocene. *Quat. Res.* **71**, 354–356 (2009).

[8] Tan, F. *et al.* Late Holocene relative sea-level records from coral microatolls in Singapore. *Sci. Rep.* **14**, 13458 (2024).

[9] Meltzner, A. J. & Woodroffe, C. D. Coral microatolls. in *Handbook of sea-level research* 125–145 (2015).

[10] Meltzner, A. J. *et al.* Half-metre sea-level fluctuations on centennial timescales from mid-Holocene corals of Southeast Asia. *Nat. Commun.* **8**, 14387 (2017).

[11] Majewski, J. M. *et al.* Extending instrumental sea-level records using coral microatolls, an example from Southeast Asia. *Geophys. Res. Lett.* **49**, e2021GL095710 (2022).

[12] Sarkawi, G. M. *et al.* A coral microatoll record of sea-level rise, interseismic deformation, and El Niño in La Union, Philippines since 1906 CE. *Mar. Geol.* **486**, 107565 (2025).

[13] Chappell, J., Chivas, A., Wallensky, E., Polach, H. A. & Aharon, P. Holocene palaeo-environmental changes, central to north Great Barrier Reef inner zone. *BMR J. Aust. Geol. Geophys.* **8**, 223–235 (1983).

[14] Mann, T. *et al.* Fossil Java Sea corals record Laurentide ice sheet disappearance. *Geology* **51**, 631–636 (2023).

[15] Majewski, J. M. *et al.* Holocene relative sea-level records from coral microatolls in Western Borneo, South China Sea. *The Holocene* **28**, 1431–1442 (2018).

[16] Leonard, N. D. *et al.* Holocene sea level instability in the southern Great Barrier Reef, Australia: high-precision U–Th dating of fossil microatolls. *Coral Reefs* **35**, 625–639 (2016).

[17] Leonard, N. D. *et al.* New evidence for "far-field" Holocene sea level oscillations and links to global climate records. *Earth Planet. Sci. Lett.* **487**, 67–73 (2018).

[18] Wan, J. X. W. *et al.* Relative sea-level stability and the radiocarbon marine reservoir correction at Natuna Island, Indonesia, since 6400 yr BP. *Mar. Geol.* **430**, 106342 (2020).

[19] Smithers, S. G. & Woodroffe, C. D. Microatolls as sea-level indicators on a mid-ocean atoll. *Mar. Geol.* **168**, 61–78 (2000).

[20] Goodwin, I. D. & Harvey, N. Subtropical sea-level history from coral microatolls in the Southern Cook Islands, since 300 AD. *Mar. Geol.* **253**, 14–25 (2008).

[21] Weil-Accardo, J. *et al.* Relative sea-level changes during the last century recorded by coral microatolls in Belloc, Haiti. *Glob. Planet. Change* **139**, 1–14 (2016).

[22] Hoarau, L. *et al.* Negative sea level anomalies with extreme low tides in the South-West Indian Ocean shape Reunion Island's fringing coral reef flats. *Ecol. Indic.* **154**, 110508 (2023).

[23] Vaughan, T. W. The results of investigations of the ecology of the Floridian and Bahaman Shoal-water corals. *Proc. Natl. Acad. Sci. U. S. A.* **2**, 95–100 (1916).

[24] Glynn, P. W. Some physical and biological determinants of coral community structure in the eastern Pacific. *Ecol. Monogr.* **46**, 431–456 (1976).

[25] Ng, C. S. L. *et al.* Enhancing the biodiversity of coastal defence structures: transplantation of nursery-reared reef biota onto intertidal seawalls. *Ecol. Eng.* **82**, 480–486 (2015).

[26] Ampou, E. E. *et al.* Coral mortality induced by the 2015–2016 El-Niño in Indonesia: the effect of rapid sea level fall. *Biogeosciences* **14**, 817–826 (2017).

[27] Mejía-Rentería, J. C., Castellanos-Galindo, G. A., Osorio-Cano, J. D. & Casella, E. Subaerial exposure of coral reefs during spring low tides in the eastern Pacific. *Bull. Mar. Sci.* **96**, 000–000 (2020).

[28] Pang, H. E., Poquita-Du, R. C., Jain, S. S., Huang, D. & Todd, P. A. Among-genotype responses of the coral *Pocillopora acuta* to emersion: implications for the ecological engineering of artificial coastal defences. *Mar. Environ. Res.* **168**, 105312 (2021).

[29] Romaine, S., Tambutté, E., Allemand, D. & Gattuso, J.-P. Photosynthesis, respiration and calcification of a zooxanthellate scleractinian coral under submerged and exposed conditions. *Mar. Biol*. **129,** 175–182 (1997).

[30] Castrillón-Cifuentes, A. L., Lozano-Cortés, D. F. & Zapata, F. A. Effect of short-term subaerial exposure on the cauliflower coral, *Pocillopora damicornis*, during a simulated extreme low-tide event. *Coral Reefs* **36**, 401–414 (2017).

[31] Dikou, A. & van Woesik, R. Survival under chronic stress from sediment load: Spatial patterns of hard coral communities in the southern islands of Singapore. *Mar. Pollut. Bull.* **52**, 1340–1354 (2006).

[32] Heery, E. C. *et al.* Urban coral reefs: Degradation and resilience of hard coral assemblages in coastal cities of East and Southeast Asia. *Mar. Pollut. Bull.* **135**, 654–681 (2018).

[33] Ng, C. S. L. *et al.* Coral community composition and carbonate production in an urbanized seascape. *Mar. Environ. Res.* **168**, 105322 (2021).

[34] Huang, D., Tun, K. P. P., Chou, L. M. & Todd, P. A. An inventory of zooxanthellate scleractinian corals in Singapore, including 33 new records. *Raffles Bull. Zool.* **22**, 69–80 (2009).

[35] Lim, L. J. W. *et al.* Diversity and distribution of intertidal marine species in Singapore. *Raffles Bull. Zool.* **68**, 396–403 (2020).

[36] Lee, Y., Lam, S. Q. Y., Tay, T. S., Kikuzawa, Y. P. & Tan, K. S. Composition and structure of tropical intertidal hard coral communities on natural and man-made habitats. *Coral Reefs* **40**, 685–700 (2021).

[37] Leslie, A. G. *et al. Singapore Geology (2021): Memoir of the Bedrock, Superficial and Engineering Geology*. Building and Construction Authority, Singapore, (2021).

[38] BCA [Building and Construction Authority]. Singapore Geology (2021): Interactive 1:50,000 Scale Map. (2021).

[39] Mapping Unit, Ministry of Defence. Singapore, 1:50,000. Series L7022, Sheet 1 to 2, Edition 7B SMU. (2005).

[40] Mapping Unit, Ministry of Defence. Singapore, 1:50,000. Series SMU 075, Sheet 1, Edition 9. (2010).

[41] Van Maren, D. S. & Gerritsen, H. Residual flow and tidal asymmetry in the Singapore Strait, with implications for resuspension and residual transport of sediment. *J. Geophys. Res. Oceans* **117**, C04021 (2012).

[42] Peng, D. *et al.* Tidal asymmetry and transition in the Singapore Strait revealed by GNSS interferometric reflectometry. *Geosci. Lett.* **10**, 39 (2023).

[43] Peng, D., Hill, E. M., Meltzner, A. J. & Switzer, A. D. Tide gauge records show that the 18.61-year nodal tidal cycle can change high water levels by up to 30 cm. *J. Geophys. Res. Oceans* **124**, 736–749 (2019).

[44] Enríquez, A. R. *et al.* Predictable changes in extreme sea levels and coastal flood risk due to long-term tidal cycles. *J. Geophys. Res. Oceans* **127**, e2021JC018157 (2022).

[45] Tkalich, P., Vethamony, P., Luu, Q.-H. & Babu, M. T. Sea level trend and variability in the Singapore Strait. *Ocean Sci.* **9**, 293–300 (2013).

[46] Luu, Q.-H., Tkalich, P. & Tay, T. W. Sea level trend and variability around Peninsular Malaysia. *Ocean Sci.* **11**, 617–628 (2015).

[47] Tan, F. *et al.* El Niño was a key driver of anomalous ocean warming in Southeast Asia in 2023. *Sci. Rep.* **15**, 16106 (2025).

[48] Natawidjaja, D. H. *et al.* Source parameters of the great Sumatran megathrust earthquakes of 1797 and 1833 inferred from coral microatolls. *J. Geophys. Res.* **111**, B06403 (2006).

[49] Tan, N. S. *et al.* Three-dimensional models of coral microatolls using structure-from-motion photogrammetry and iPhone LiDAR scanning: A fast, reproducible method for collecting relative sea-level data in the field. (Under review).

[50] Wessel, P. *et al.* The Generic Mapping Tools Version 6. *Geochem. Geophys. Geosystems* **20**, 5556–5564 (2020).

[51] Codiga, D. L. *Unified Tidal Analysis and Prediction Using the UTide Matlab Functions. 481 Technical Report 2011-01.* Graduate School of Oceanography, University of Rhode Island, Narragansett, RI, Narragansett, RI, 2011.

[52] Tan, F. *et al.* Holocene relative sea-level histories of far-field islands in the mid-Pacific. *Quat. Sci. Rev.* **310**, 107995 (2023).

[53] Cooper, T. F., De'ath, G., Fabricus, K. E. & Lough, J. M. Declining coral calcification in massive *Porites* in two nearshore regions of the northern Great Barrier Reef. *Glob. Change Biol.* **14**, 529–538 (2008).

[54] Scoffin, T. P., Tudhope, A. W., Brown, B. E., Chansang, H. & Cheeney, R. F. Patterns and possible environmental controls of skeletogenesis of *Porites lutea*, South Thailand. *Coral Reefs* **11**, 1–11 (1992).

[55] Tanzil, J., Brown, B. E., Tudhope, A. W. & Dunne, R. P. Decline in skeletal growth of the coral *Porites lutea* from the Andaman Sea, South Thailand between 1984 and 2005. *Coral Reefs* **28**, 519–528 (2009).

[56] van Woesik, R., Golbuu, Y. & Roff, G. Keep up or drown: adjustment of western Pacific coral reefs to sea-level rise in the 21st century. *R. Soc. Open Sci.* **2**, 1150181 (2015).

[57] Lim, J. T. Y. *et al.* Investigation of an ongoing sequence of coral microatoll diedowns in Singapore (2020-2024?). in *AGU Fall Meeting Abstracts* PP45B-1110 (2021).

[58] Poquita-Du, R. C., Du, I. P. M. & Todd, P. A. EmerSense: A low-cost multiparameter logger to monitor occurrence and duration of emersion events within intertidal zones. *HardwareX* **14**, e00410 (2023).

[59] Poquita-Du, R. C., Huang, D. & Todd, P. A. Genome-wide analysis to uncover how *Pocillopora acuta* survives the challenging intertidal environment. *Sci. Rep.* **14**, 8538 (2024).

[60] Weil-Accardo, J. *et al.* Two hundred thirty years of relative sea level changes due to climate and megathrust tectonics recorded in coral microatolls of Martinique (French West Indies). *J. Geophys. Res. Solid Earth* **121**, 2873–2903 (2016).

[61] Komori, J., Gautam, R., Tan, N. S. & Meltzner, A. J. Simulation-based approach for reconstructing past relative sea-level changes using coral microatolls. *Geomorphology* **473**, 109609 (2025).

[62] Lorscheid, T. & Rovere, A. The indicative meaning calculator – quantification of paleo sea-level relationships by using global wave and tide datasets. *Open Geospatial Data Softw. Stand.* **4**, 10 (2019).

[63] Anthony, K. R. N. & Kerswell, A. P. Coral mortality following extreme low tides and high solar radiation. *Mar. Biol.* **151**, 1623–1631 (2007).

[64] Dunne, R. P., Brown, B. E., Spencer, T. & Woodworth, P. L. Coral bleaching at Low Isles during the 1928–1929 Great Barrier Reef Expedition. *Coral Reefs* **41**, 1595–1610 (2022).

[65] Tan, K. S., Acerbi, E. & Lauro, F. M. Marine habitats and biodiversity of Singapore's coastal waters: A review. *Reg. Stud. Mar. Sci.* **8**, 340–352 (2016).

[66] McCarthy, O. S., Winston Pomeroy, M. & Smith, J. E. Corals that survive repeated thermal stress show signs of selection and acclimatization. *PLoS ONE* **19**, e0303779 (2024).

[67] González-Barrios, F. J., Estrada-Saldívar, N., Pérez-Cervantes, E., Secaira-Fajardo, F. & Álvarez-Filip, L. Legacy effects of anthropogenic disturbances modulate dynamics in the world's coral reefs. *Glob. Change Biol.* **29**, 3285–3303 (2023).

[68] Humanes, A. *et al.* Selective breeding enhances coral heat tolerance to marine heatwaves. *Nat. Commun.* **15**, 8703 (2024).

[69] Brown, B. E., Dunne, R. P., Phongsuwan, N., Patchim, L. & Hawkridge, J. M. The reef coral *Goniastrea aspera*: a 'winner' becomes a 'loser' during a severe bleaching event in Thailand. *Coral Reefs* **33**, 395–401 (2014).

[70] Lai, S., Loke, L. H. L., Hilton, M. J., Bouma, T. J. & Todd, P. A. The effects of urbanisation on coastal habitats and the potential for ecological engineering: A Singapore case study. *Ocean Coast. Manag.* **103**, 78–85 (2015).

[71] Crameri, F. Scientific colour maps. https://doi.org/10.5281/ zenodo.1243862 (2018).

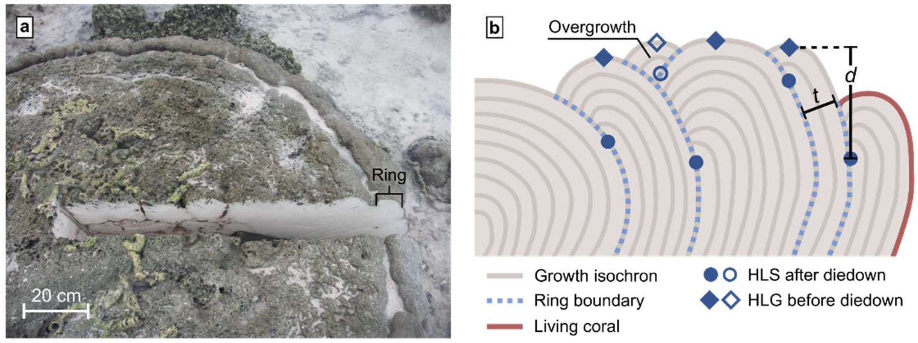

Figure 1 Surface morphology and internal structure of coral microatolls. **(a)** Photograph of a microatoll[8] showing the internal ring and overgrowth boundaries where a slab has been removed. Photo credit: A.J.M. **(b)** Schematic radial cross section of a microatoll. Filled symbols for HLG (highest level of growth) and HLS (highest level of survival) used for in-sequence rings and hollow symbols used for overgrowth. Note that the HLS and HLG of the overgrowth lie at a slightly higher elevation than the coeval in-sequence ring. *d*: Diedown magnitude; *t*: Ring thickness.

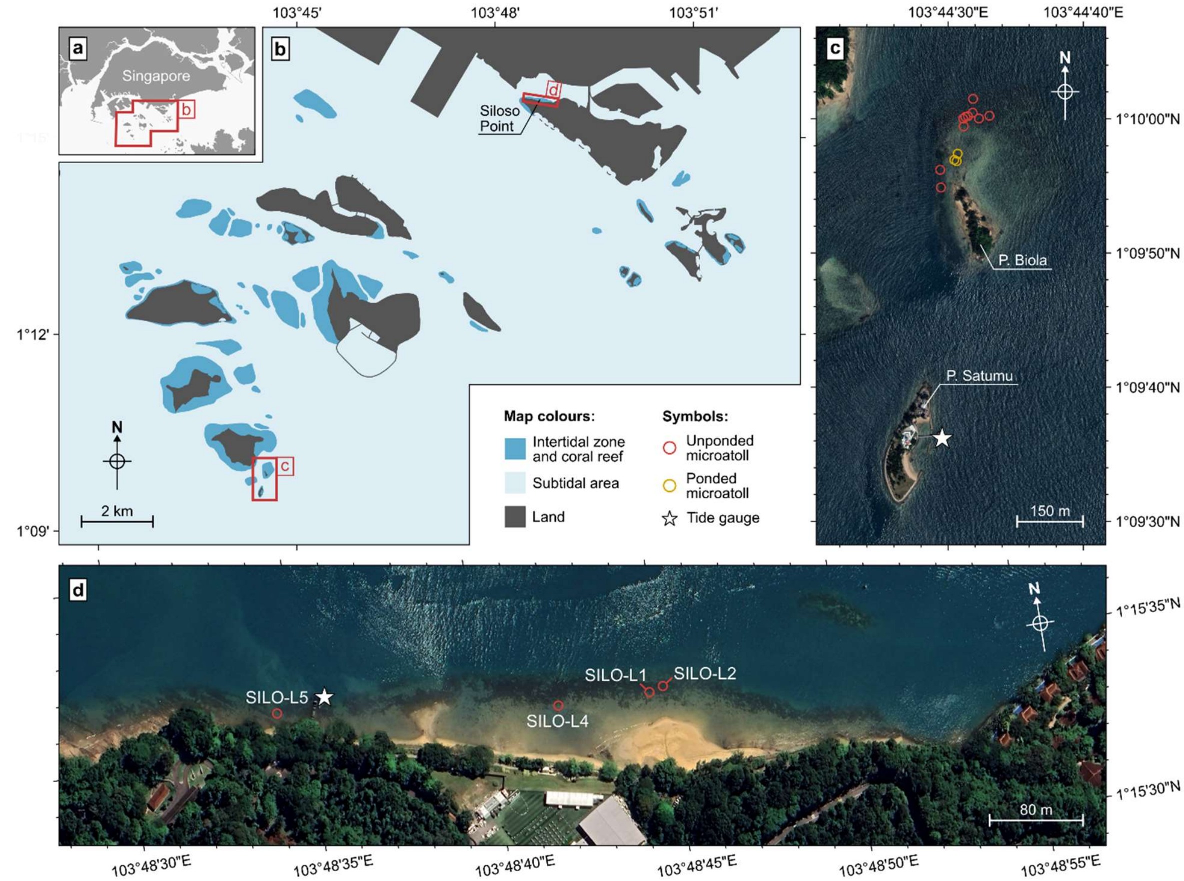

Figure 2 Locations of living microatolls and tide gauges used in this study. (a) Map of Singapore and surroundings with location of panel (b) highlighted. **(b)** Islands of southern Singapore showing intertidal reef areas adapted from ref.[70], field surveys and Google Earth imagery. 'Siloso Point' refers to the reef site first described by ref.[8]. **(c)** Locations of the living microatolls surveyed at the Biola reef and the Raffles Lighthouse tide gauge on Pulau Satumu. P. = Pulau (Island). Image source: Google Earth (Imagery date: 10th February 2018). **(d)** Map of the Siloso Point reef showing the locations of the tide gauge and the living microatolls used in this study. Image source: Google Earth (Imagery date: 2nd April 2024). Figure produced using the Generic Mapping Tools v.6[50].

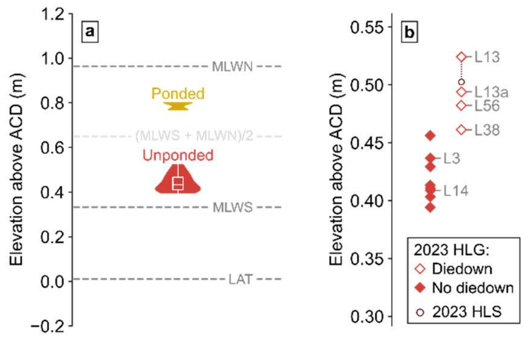

Figure 3 Highest level of growth (HLG) of microatolls on the Biola reef. (a) Violin plots of HLG for surveyed *Porites* spp. microatolls relative to admiralty chart datum (ACD). Boxplot shows median, first quantile and third quantile. Ponded microatolls are those in the highest area of moated water. LAT: Lowest astronomical tide; MLWS: Mean low water springs; MLWN: Mean low water neaps. **(b)** Highest 2023 HLG per coral for unponded microatolls in panel (a) and highest surveyed post-diedown 2023 HLS for BIOL-L13. Microatolls discussed in the text are labelled. Note that a 2.7 cm uncertainty from surveying the tide-gauge benchmark applies to the value of ACD, which is a correlated error for all microatoll elevation measurements.

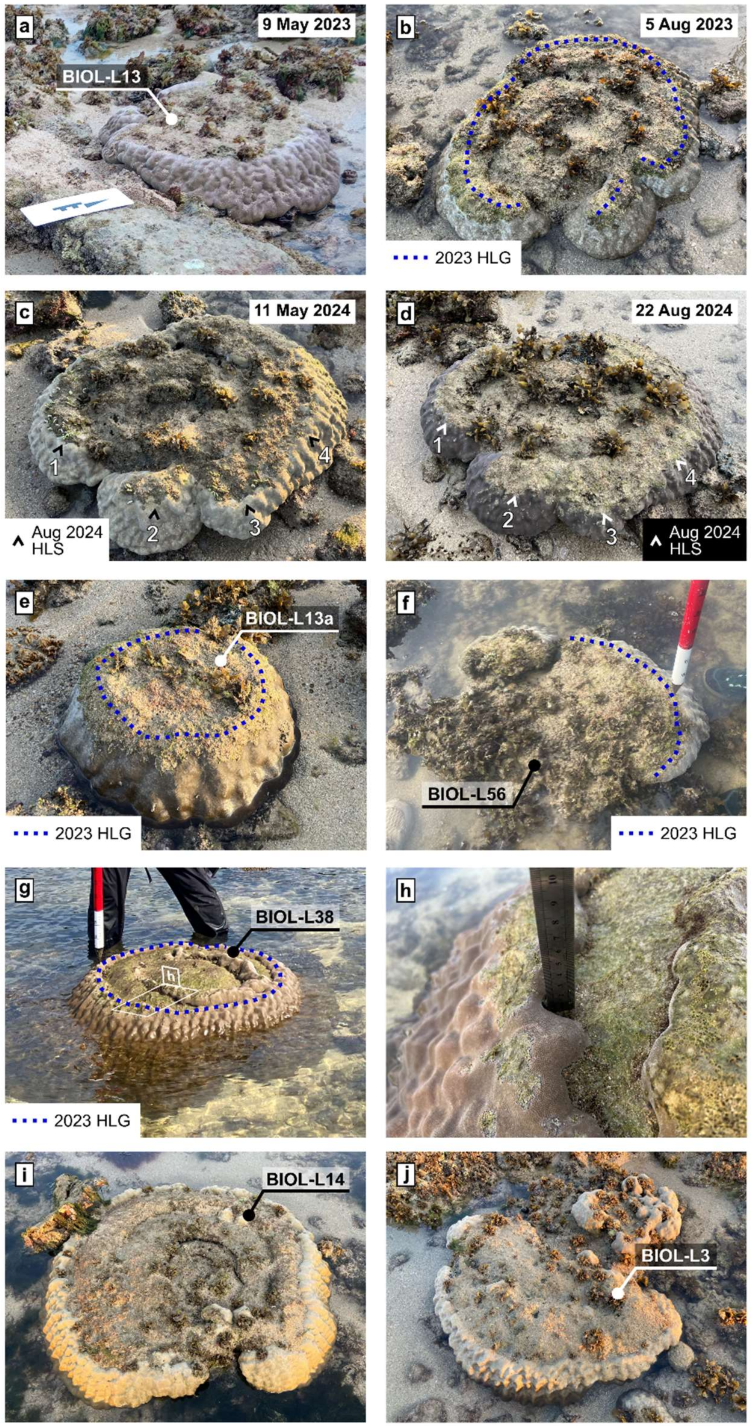

Figure 4 Photographs of selected corals analysed in this study. Microatoll BIOL-L13: **(a)** before and **(b)** after the diedown in mid-2023 (pre-diedown HLG indicated with a dotted line); **(c)** bleached in May 2024; **(d)** as observed in August 2024. Arrows with equivalent numbers in (c) and (d) point to the same area of the microatoll before and after the 2024 diedown. **(e)** Microatoll BIOL-L13a with pre-2023 diedown HLG indicated with a dotted line. Photograph taken 5th August 2023. **(f)** BIOL-L56. Photograph taken 5th August 2023 after the mid-2023 diedown. **(g)** BIOL-L38 on 7th July 2023. Location of close-up photograph in panel (h) highlighted. **(h)** BIOL-L38 on 2 September 2023 showing recent partial mortality on the top of the microatoll's outer rim (to the left of the rule in the

photograph). **(i)** BIOL-L14 on 11th May 2024, showing the coral fully exposed and bleached, but with no signs of recent partial mortality. **(j)** BIOL-L3 on 23rd April 2023. Additional photographs of these microatolls and other surveyed corals can be found in Supplementary Figure S5. Photo credits: (a-f,h,i) J.Q.S., (g,j) A.J.M.

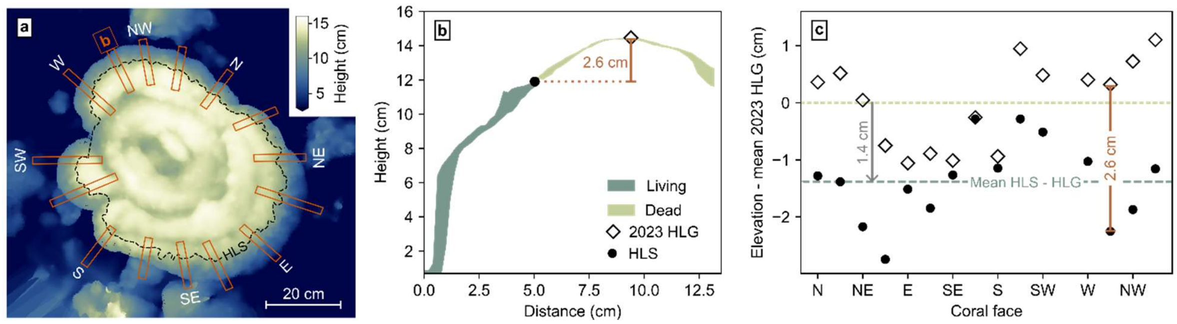

Figure 5 BIOL-L13's highest level of growth (HLG) in 2023 and highest level of survival (HLS) after the mid-2023 diedown. **(a)** Digital surface model of BIOL-L13 generated from a LiDAR point cloud captured on 5th August 2023. Elevations are given as height above the reef substrate within the LiDAR scan area, and absolute magnitudes are arbitrary. Rectangles: swath profile areas used to measure pre-diedown HLG and post-diedown HLS annotated according to orientation. Swath profile from the WNW face shown in panel **(b)** as an example of the HLG and HLS measurement. **(c)** Relative elevations of pre-diedown HLG and post-diedown HLS elevations measured from all swath profiles. Details of the LiDAR scan processing and uncertainty estimation can be found in the Supplementary Information. This figure uses the Scientific Color Map *davos*[71].

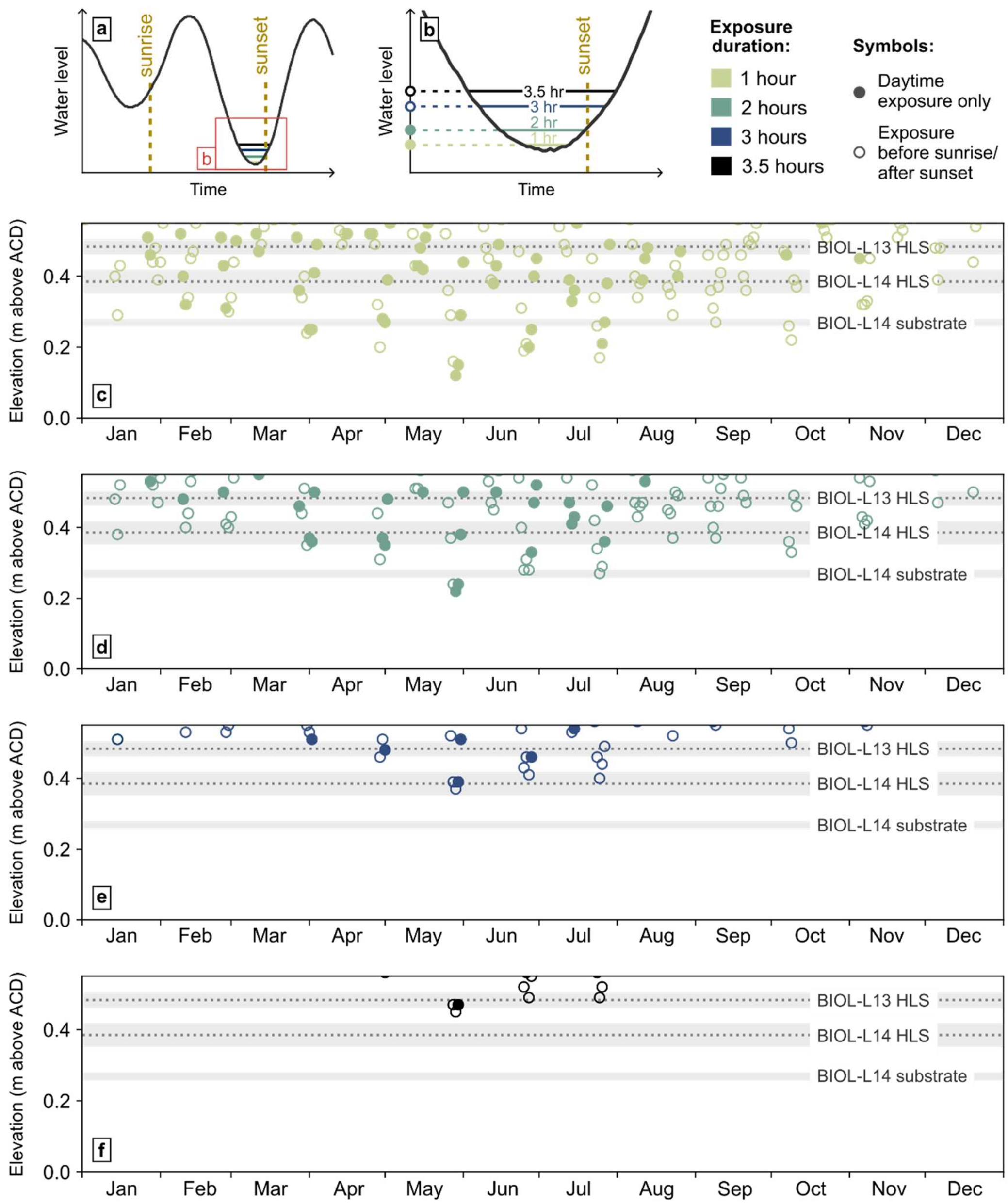

Figure 6 Lowest elevation subaerially exposed for a continuous 1-, 2-, 3- or 3.5-hour period per day during 2021 and estimated HLS of BIOL-L14 and BIOL-L13. (a) Example of daily water level measured in a mixed semi-diurnal tidal regime. Lowest elevation continuously exposed for a 1, 2-, 3-, or 3.5-hour period highlighted using coloured lines. **(b)** The low-tide period of the data shown in panel (a). **(c)** Daily lowest elevation above chart datum exposed for a one-hour time interval during the year 2021. Filled circles denote low tides that occurred entirely between sunrise and sunset, while hollow circles represent exposure that occurred partially or wholly before sunrise or after sunset. HLS: highest level of survival for the most recent diedown. **(d,e,f)** As for panel **(c)** but showing the lowest elevation that was exposed for 2, 3 or 3.5 hours, respectively. ACD: Admiralty Chart Datum.

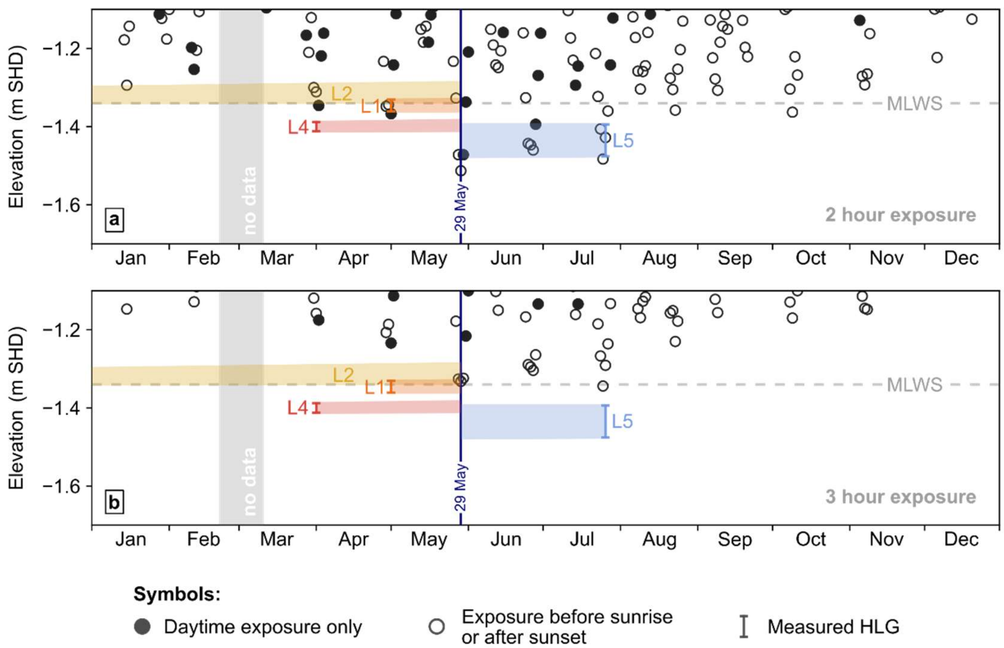

Figure 7 Lowest elevation on the Siloso Point reef exposed for continuous (a) 2-, or (b) 3-hour period during 2021 and extrapolated HLG of Siloso Point microatolls. Hollow symbols indicate that at least part of the daily exposure occurred before sunrise or after sunset. The grey shaded area represents a data gap in the tide-gauge record. HLG (highest level of growth) vertical lines show the full range (minimum to maximum) of living rim elevations measured using the total station on that survey day. HLG is extrapolated to 29th May 2021. SHD: Singapore Height Datum.

Supplementary Information for

'Coral microatoll partial mortality after multi-hour subaerial exposure: Implications for relative sea-level studies'

by Jennifer Quye-Sawyer, Jing Ying Yeo, Wan Lin Neo, Fangyi Tan, Jun Yu Puah & Aron J. Meltzner

Contact: j.quye.sawyer@gmail.com

Contents

Abbreviations

ACD:	Admiralty Chart Datum. A marine datum based upon the lowest recorded water levels.
SHD:	Singapore Height Datum. A land survey datum based upon historical mean sea level.
HLG:	Highest level of growth (of microatoll's outer living rim).
HLS:	Highest level of survival of living coral after a diedown

All times are Singapore Standard Time (UTC+8).

1. Data processing for the Siloso Point tide gauge

We recorded water levels at the Siloso Point site using ONSET HOBO U20-001-04-Ti pressure-sensor tide gauges ('loggers') attached to a disused jetty. In this study, we use data collected from January 2021 to June 2024. The data collection and data processing protocols can be found in Tan et al. (2024) and are summarized below.

Water level recordings were made in 2-, 4-, 5- or 6-minute intervals from loggers installed in a series of mostly overlapping deployments (one pair of sequential deployments did not overlap). The overlap periods ranged from 30 minutes to 27 days. The elevation of each logger was surveyed using a total station at times of installation and removal, and the elevations of all logger deployments were tied to the same reference frame as our coral surveys using benchmarks at the Siloso site. The average logger elevation was used if more than one reliable elevation measurement was obtained during a deployment. In addition to repeat total station surveys of the logger elevation, we repeatedly measured from the logger to a fixed point on the jetty above to check for physical movement of the sensor during the deployment. No loggers are inferred to have moved from their installation height.

We compensated each logger deployment using barometric pressure recorded by an ONSET HOBO U20L-04 pressure sensor and the distance from the water surface to the logger sensor at a specific time measured using a tape measure (henceforth a 'tape-measure measurement'). We also measured water level on the reef directly with a graduated rod and surveyed the elevation of the reef substrate at this point using the total station (a 'graduated-rod measurement'). For the graduated rod measurements, we recorded water level in five-second increments for two minutes and calculated the mean water level for this two-minute period. We repeated the tape-measure measurements and graduated-rod measurements several times during each logger deployment and calibrated the logger output by minimizing the residuals between field measurements and logger readings. The calibrations were performed independently for each deployment, except for the 1st August–11th October 2022 deployment as we did not obtain any reliable field measurements during this period. For the 1st August–11th October 2022 deployment, we shifted the data recorded by the1st August–11th October logger to minimize the misfit between the two deployments in the 27th September to 11th October 2022 overlap period.

Once calibrated, all logger deployments were combined, and one of the logger outputs from each overlap period was removed. The deployment with the smaller residuals between logger output and tape-measure / graduated-rod measurements was retained. Post-calibration residuals between the water levels recorded by the loggers and our field measurements have a standard deviation of 2.7 cm (Figure S1).

We used the repeat tape-measure measurements and graduated-rod measurements to check for instrument drift within each deployment. Where necessary, we validated the logger's water level readings using a separate tide gauge installed at a nearby site (St John's Island) and photographs of coral emersion/submersion on the Siloso Point reef.

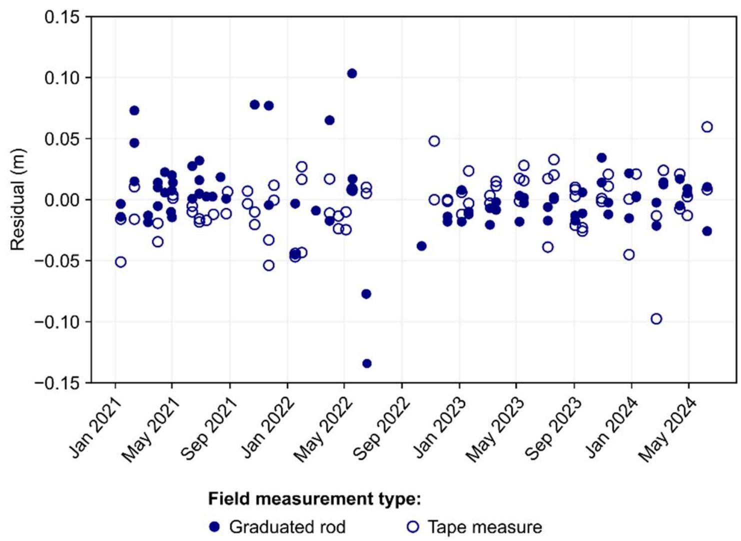

Figure S1. Difference between water levels recorded by the tide gauge and field measurements of water level at the Siloso Point site. Residuals were calculated after compensation and after refining the calibration by minimizing the misfit between field observations and logger recordings.

Two deployments are inferred to have been affected by instrumental drift: 10th February–10th March 2021 and 17th June –17th August 2022.

The 10th February–10th March 2021 deployment recorded unexpectedly low water levels at the end of February. This logger recorded water levels lower than −1.50 m SHD between 5:40 pm and 7:00 pm on 27th February 2021, though these recorded water levels are inconsistent with the magnitude of exposure observed on the living corals at this time. For example, SILO-L1 was exposed to the level of its HLG (approximately -1.35 m SHD) between 5:50 pm and 6:00 pm on 27th February 2021 (Figure S2a), implying that the true water level was ≈15 cm higher than the value concurrently recorded by the tide gauge. In contrast, the -1.49 m SHD water level recorded by a subsequent (and not apparently drifting) logger deployment at the Siloso site on 1st May 2021 is consistent with the exposure of this microatoll to ~10 cm below HLG at this time (Figure S2b). These observations lead us to believe that the end of February water level readings are incorrect.

Due to a delay in installing the next logger, the 10th February–10th March 2021 deployment did not overlap in time with the following deployment that started on 11th March 2021. Therefore, we cannot use an overlap period to deduce if the anomalously low water level readings occurred for just a few days at the end of February 2021 or if the apparent drift continued until the end of the deployment. Nonetheless, from 20th February to the end of the deployment on 10th March 2021, the Siloso Point logger recorded a larger net decrease in daily average water level than was recorded by a logger installed in a similar setup at St John's Island (Figures S2c, S3). While sea-level anomalies are spatially complex in the Singapore Straits, so the different trends between the two sites may represent real conditions, we removed the Siloso Point tide gauge data from 20th February 2021 to 10th March 2021 in case the logger was drifting for all of this time.

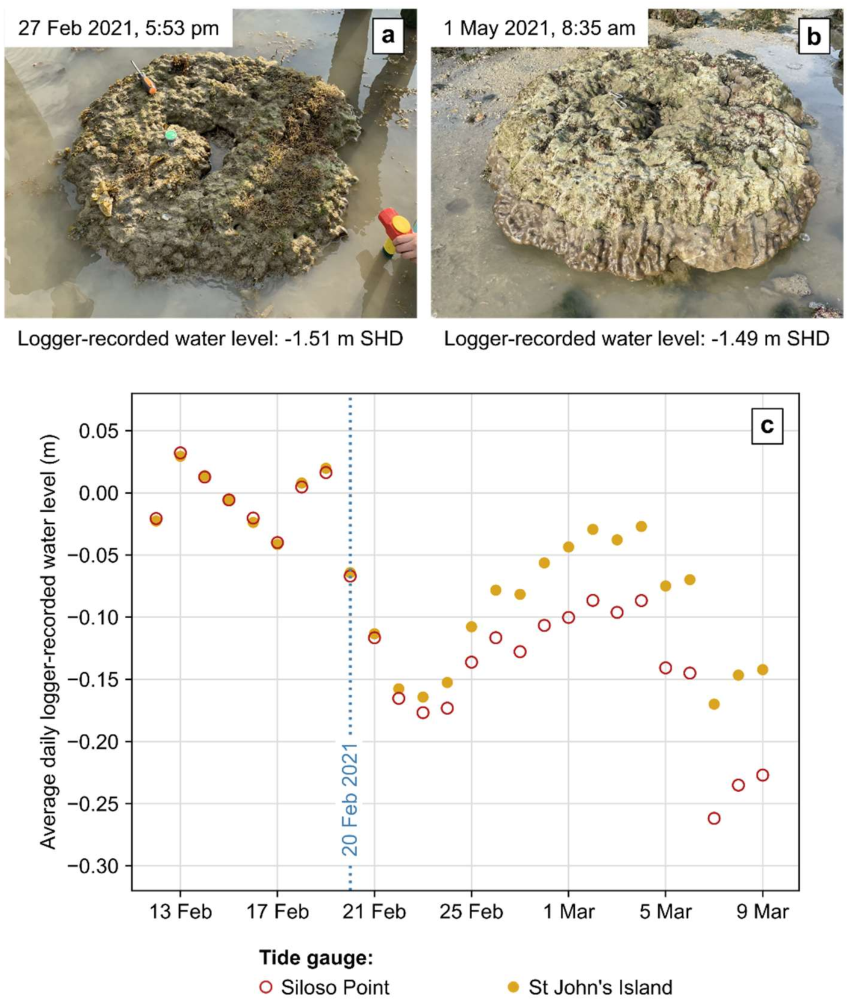

Figure S2. (a) Photograph of SILO-L1 taken on 27th February 2021 and (b) the same coral on 1st May 2021. (c) Daily mean water level recorded at simultaneous tide-gauge deployments on the Siloso reef and at St John's Island (location shown on Fig. S3). Data have been vertically shifted so the average water levels over the first seven days are set to zero for both deployments. The logger at Siloso Point was inferred to have started drifting at some time after 20th February 2021 when average water levels from loggers at these sites start to diverge.

The logger deployment of 17th June –17th August 2022 recorded a ~10 cm drop in mean daily water level between 24th and 26th July 2022. Daily mean sea-level trends did not match those of the next deployment during the overlap period from 1st August to 17th August 2022. Therefore, due to suspected instrument malfunction from 24th July, the entire 17th June–17th August 2022 deployment was removed from the tide-gauge time series.

We also compared the monthly average water levels from the Siloso tide gauge record to monthly average water levels recorded at nearby permanent tide gauges to investigate the reliability of our combined water level time series from all loggers (Figure S3). Data for the permanent tide gauges were downloaded from the Permanent Service for Mean Sea Level (PSMSL). We find that the monthly average water levels at the Siloso tide gauge closely track the trends and magnitudes measured by at least one of the permanent tide gauges – except for July to August 2021, where all permanent tide gauges recorded an increase in monthly mean water level (Figure S4).

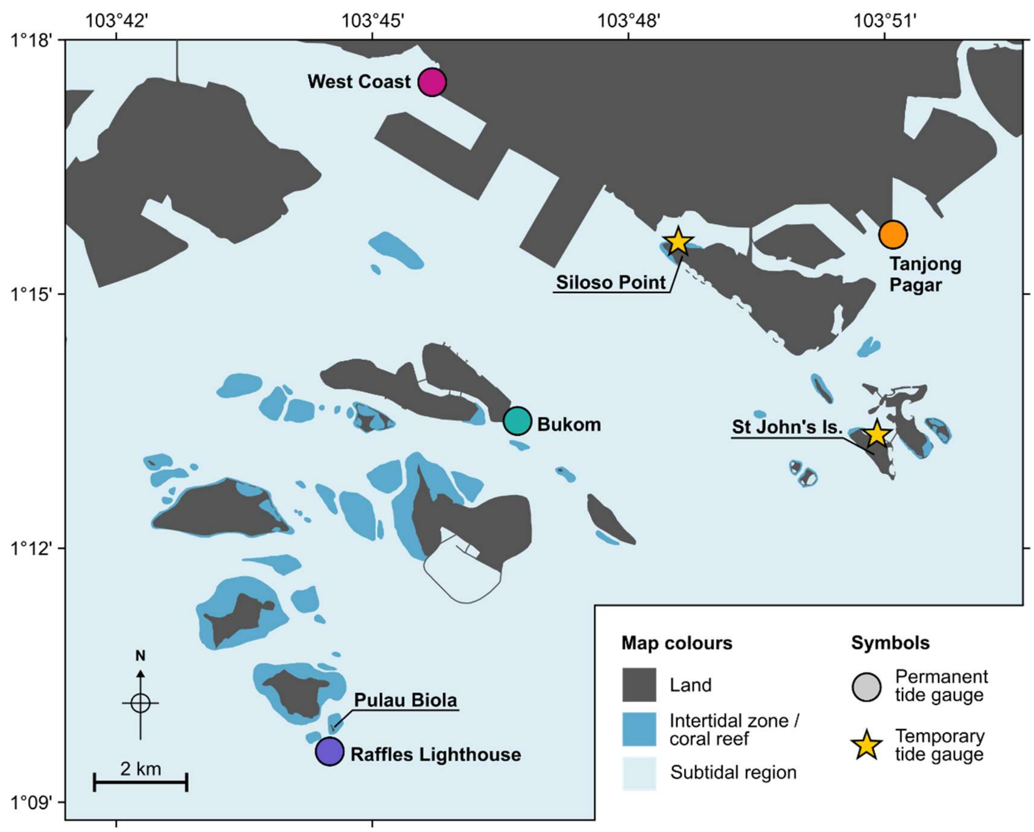

Figure S3. Locations of the temporary tide gauge at the Siloso Point reef and St John's Island and nearby permanent tide gauges. Colors for permanent tide gauges correspond to those used in Fig. S4.

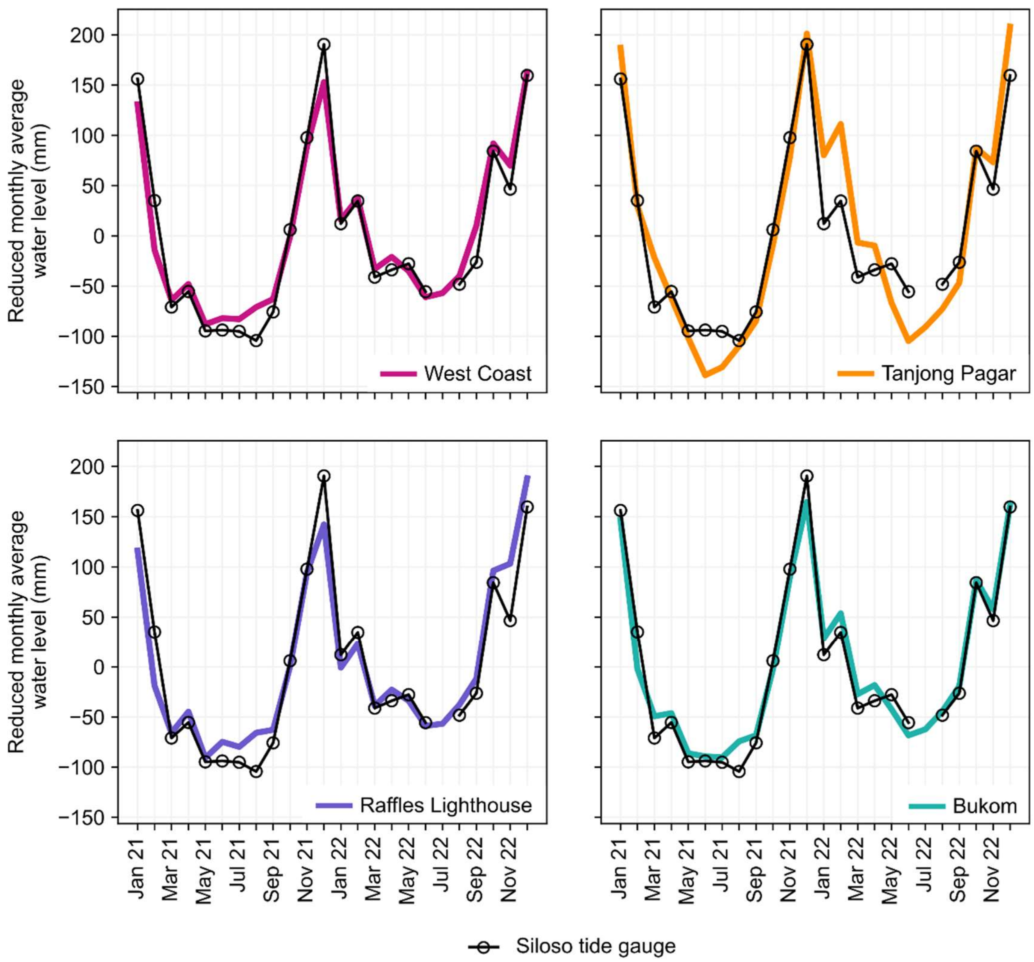

Figure S4. Monthly mean water levels during 2021 and 2022 recorded by the Siloso tide gauge and proximal permanent tide gauges. For ease of comparison between sites, each tide gauge's mean monthly average water level was subtracted from all values. Tide gauge locations shown in Fig. S3.

2. Photographs and elevations of the Biola reef microatolls

BIOL-L13

BIOL-L13a

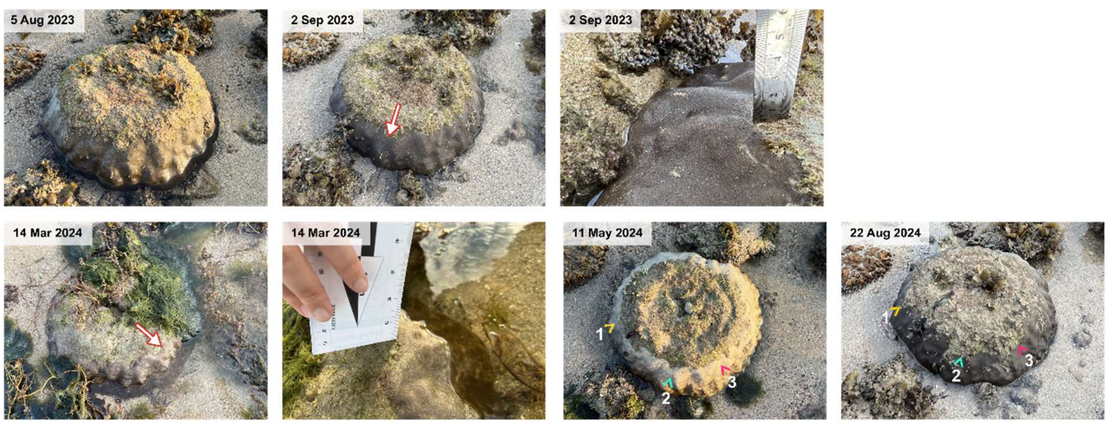

BIOL-L38

Figure S5. Photographs of *Porites* spp. microatolls on the Biola reef. Arrows with a red outline point to the position of the scale in the following close-up photograph. Arrow on the white plastic scale bar (seen on BIOL-L13 in the 2nd Sept. 2023 photograph, for example) has a length of 10 cm and points north. For BIOL-L13a, the numbered chevrons point to the same position on the coral before and after the mid-2024 diedown. A high-resolution version of this figure is available in the Zenodo repository.

BIOL-L14

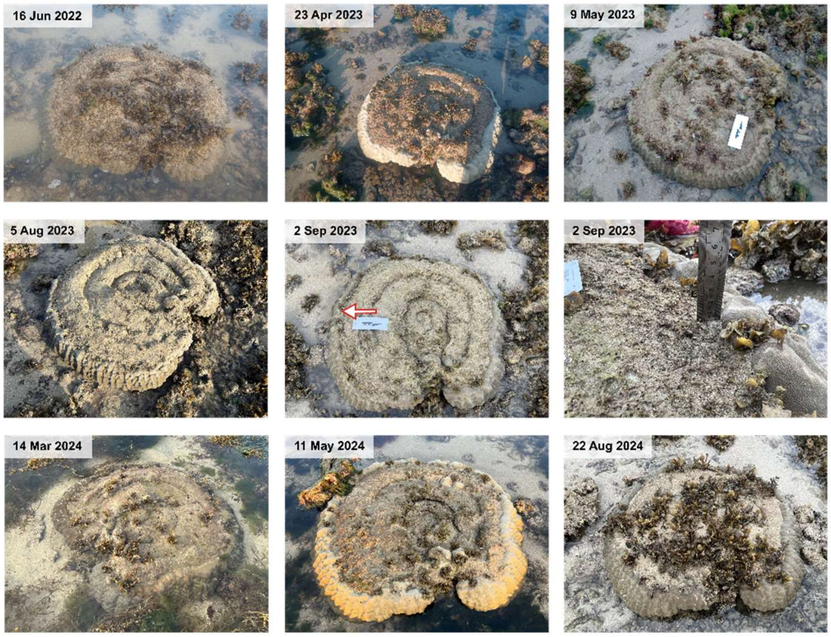

BIOL-L3

BIOL-L50

Figure S5 (continued)

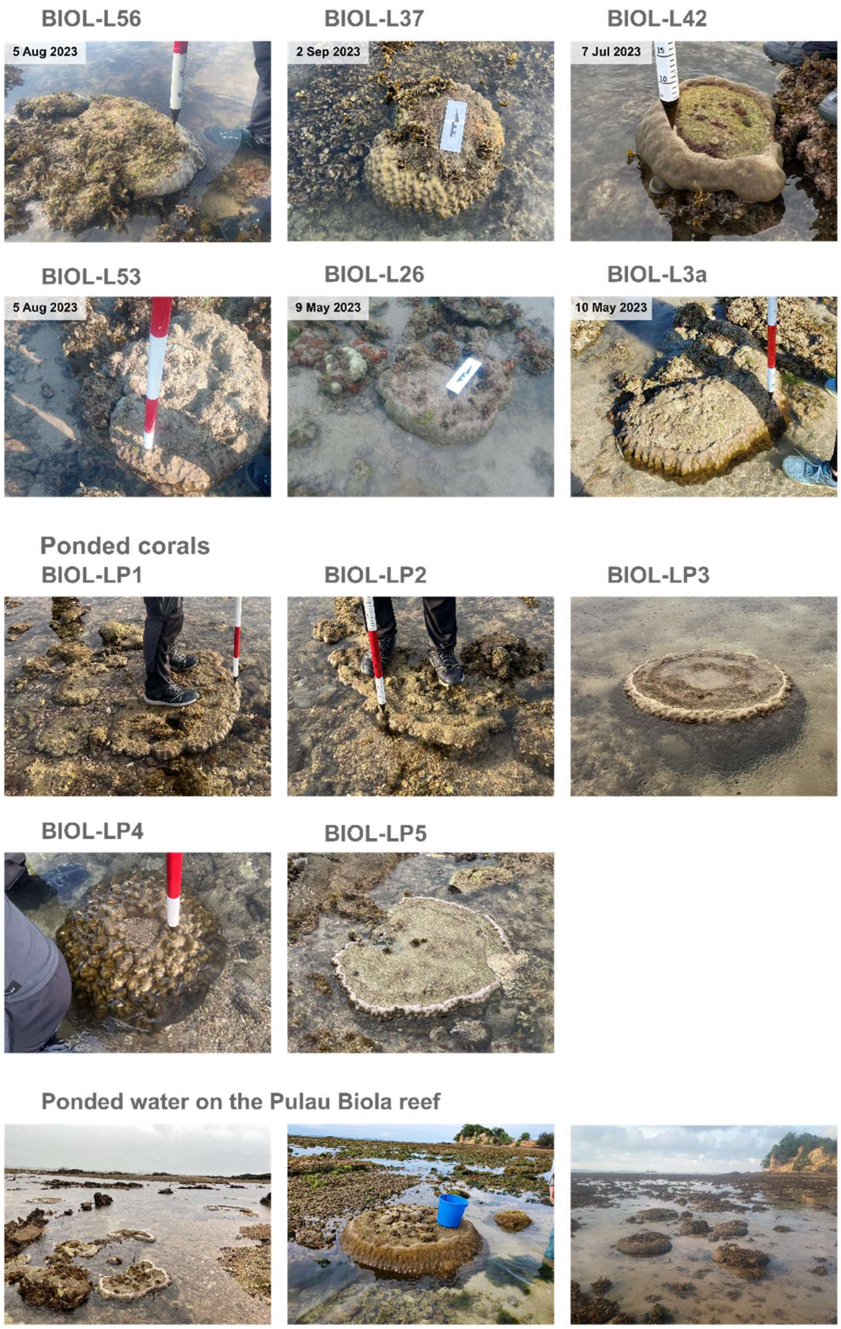

Figure S5 (continued)

Table S1. Locations of the Biola reef unponded microatolls used in this study and elevations of the highest part of the microatolls' living outer rims in 2023. ACD: Admiralty chart datum for the Raffles Lighthouse tide gauge. Value for ACD is based upon the mean of three repeat measurements of the tide-gauge benchmark. The repeat measurements of the tide-gauge benchmark had a standard deviation of 2.7 cm, which is a correlated uncertainty for all surveyed microatolls. For those corals that died down in 2023, the highest part of the outermost dead ring was surveyed shortly after the mid-2023 diedown.

Coral ID	**Latitude**	**Longitude**	**Elevation (m above ACD)**	**Diedown in 2023?**
BIOL-L3	1.16636	103.74268	0.4368	No
BIOL-L3a	1.16636	103.74268	0.4108	No
BIOL-L13	1.16651	103.74199	0.5243	Yes
BIOL-L13a	1.16651	103.74199	0.4940	Yes
BIOL-L14	1.16672	103.74208	0.4088	No
BIOL-L26	1.16667	103.74230	0.4033	No
BIOL-L37	1.16525	103.74152	0.4563	No
BIOL-L38	1.16561	103.74151	0.4613	Yes
BIOL-L42	1.16708	103.74218	0.4133	No
BIOL-L50	1.16671	103.74202	0.4293	No
BIOL-L53	1.16679	103.74217	0.3943	No
BIOL-L56	1.16667	103.74198	0.4823	Yes

Table S2. Locations of the Biola reef ponded microatolls used in this study and elevations of the highest part of the microatolls' living outer rims and outermost dead ring. ACD: Admiralty chart datum for the Raffles Lighthouse tide gauge. Value for ACD is based upon the mean of three repeat measurements of the tide-gauge benchmark. The repeat measurements of the tide-gauge benchmark had a standard deviation of 2.7 cm, which is a correlated uncertainty for all surveyed microatolls. Elevations surveyed in August 2024.

Coral ID	**Latitude**	**Longitude**	**Elevation (m above ACD)**	
			Living rim	**Outermost dead ring**
BIOL-LP1	1.16594	103.74186	0.782	0.773
BIOL-LP2	1.16594	103.74186	0.778	0.804
BIOL-LP3	1.16582	103.74180	0.797	0.795
BIOL-LP4	1.16582	103.74180	0.781	0.767
BIOL-LP5	1.16579	103.74184	0.796	0.801

3. Photographs of the mid-2021 diedown on Siloso Point microatolls

For the coral microatolls at Siloso Point, we used photographs of the living outer rim to deduce whether a diedown occurred between end May and mid- June 2021 (Figure S6). We estimated diedown magnitude on SILO-L1, SILO-L2 and SILO-L4 using equivalent features in paired photographs from May and June 2021 (Figure S6). On 27th June 2021, SILO-L5's living outer rim appears to be a few centimeters thick and unbleached. There is no evidence of sediment covering the crest of the outer rim. Therefore, we infer that SILO-L5 did not have a diedown in late May or June 2021 (Figure S6).

From July to October 2021, the upper part of SILO-L1, -L2 and L4's outer rims that had been alive at the start of the year became progressively covered in thicker mud, sand and vegetation (Figure S7). The thicker mud and vegetation on these microatolls extended down to the top of the living outer rim of coral, suggesting that several months had passed since the partial mortality event and that no new diedown has occurred since end May and mid- June 2021.

Figure S6. Photographs of *Porites* spp. microatolls at Siloso Point before and after the mid-2021 diedown. Arrow heads touch the post-diedown HLS on SILO-L1 -L2 and -L4's images. Arrows of the same colour point to the same location in the paired before- and after-diedown photographs.

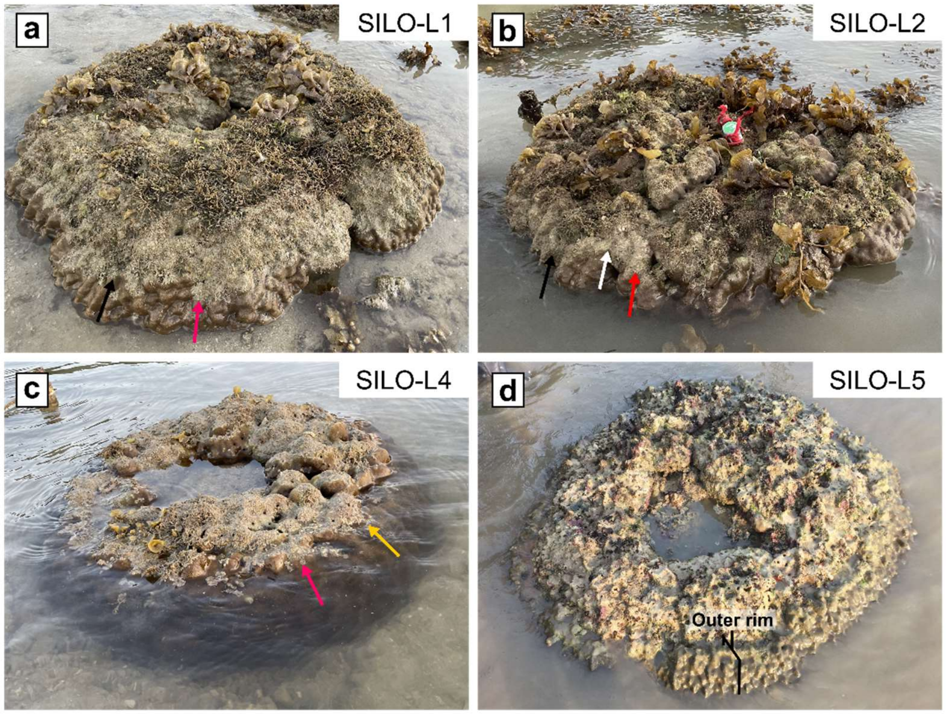

Figure S7. Photographs of microatolls SILO-L1, SILO-L2, SILO-L4 and SILO-L5 at Siloso Point several months after the mid-2021 diedown. Photographs in panels **(a–c)** were taken on 8th October 2021. Photograph in panel **(d)** was taken on 26th July 2021 (Photo credit: Joanne Lim). Arrows point to the same features as in Fig. S6 where these features can be seen in panels (a–c). SILO-L1 has an average radius of 59 cm, SILO-L2 has an average radius of 40 cm, SILO-L4 has an average radius of 27 cm and SILO-L5 has an average radius of 60 cm.

4. Microatoll digital surface models and swath profiles

Point clouds were captured in August 2023 using the inbuilt iPhone LiDAR scanner and Scaniverse application and exported in .ply and .obj format. High scan accuracy should be obtained since all microatoll dimensions (height × width × length) are greater than 10 cm (Luetzenburg et al., 2021), yet the microatoll's small size and easy accessibility from all angles facilitates quick LiDAR scanning that limits the potential for unwanted drift (Tan et al., under review; Luetzenburg et al., 2024). Point cloud density calculated using CloudCompare's 'Surface Density' tool is shown in Figures S8, S9, and S10.

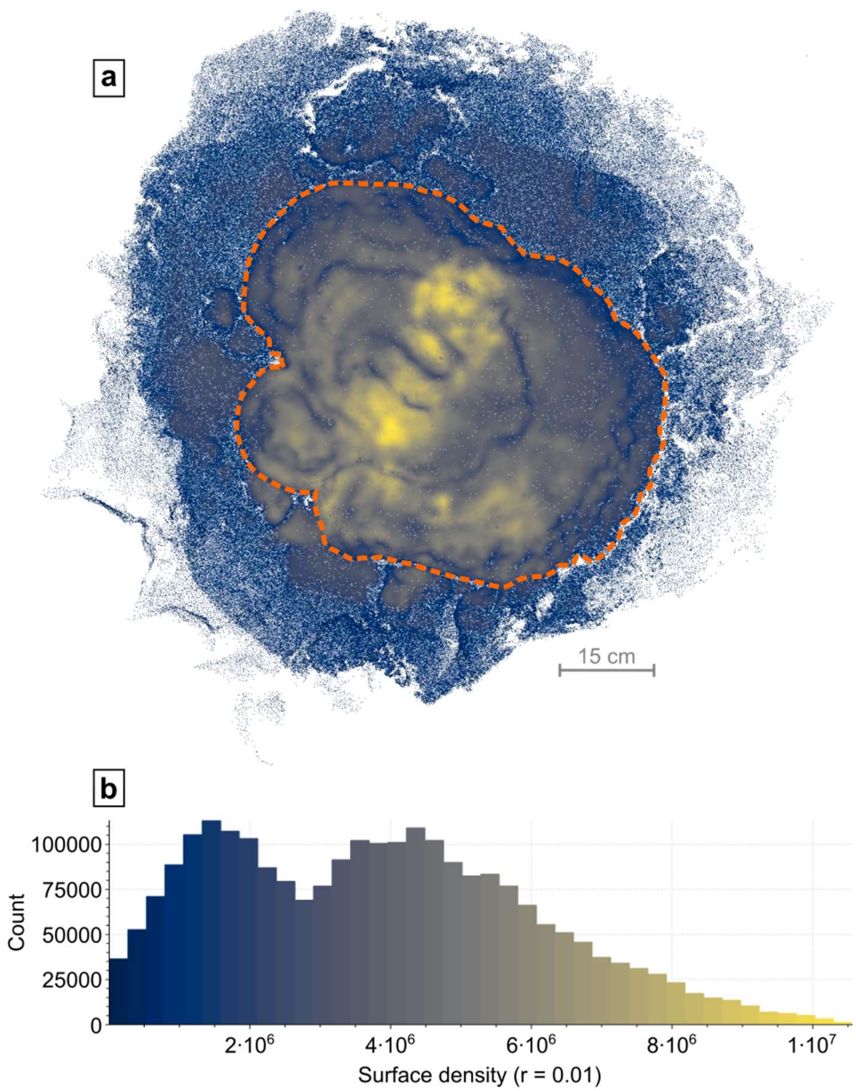

Figure S8. LiDAR point cloud density for BIOL-L13. (a) Map view of surface density (in points/m^2) calculated within a 0.01 m radial distance of each point. Calculations performed on the un-interpolated point cloud. Outer perimeter of the microatoll is shown with a dashed orange line. **(b)** Histogram of point cloud density for BIOL-L13.

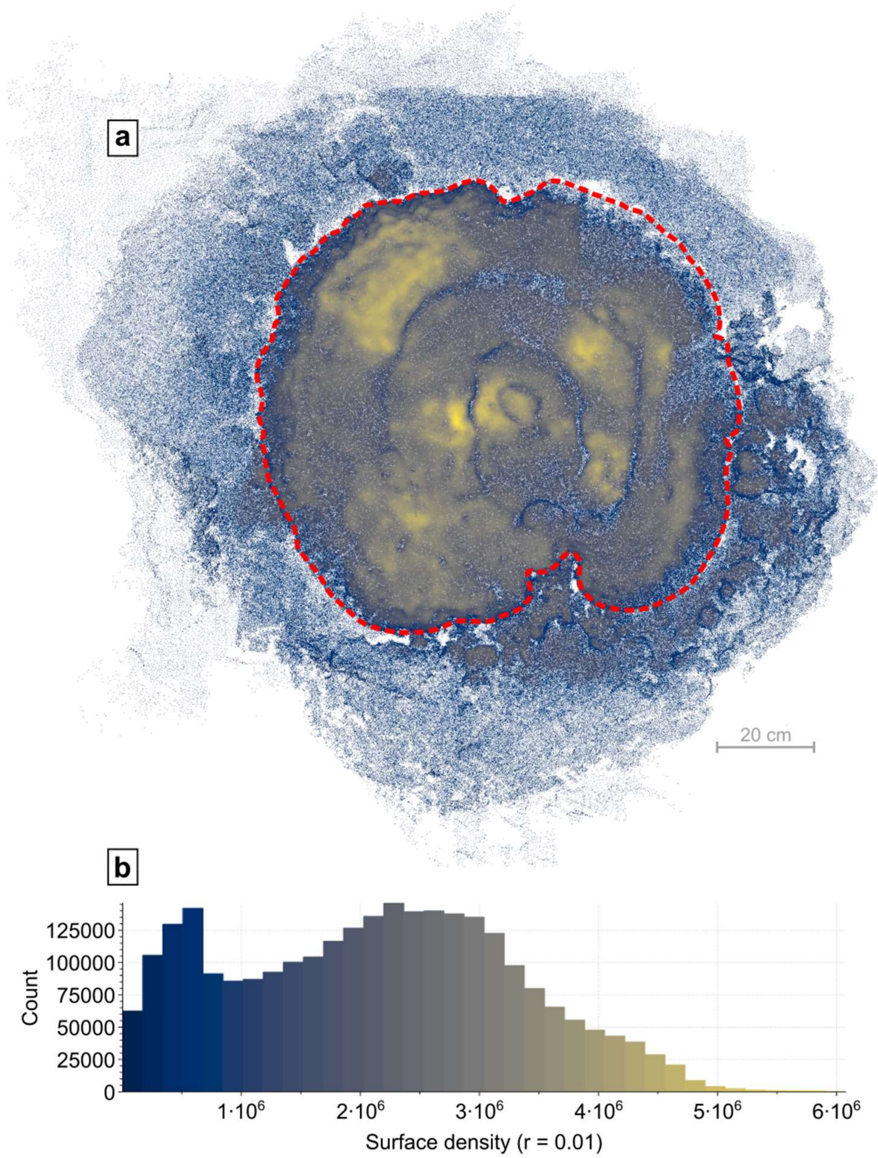

Figure S9. LiDAR point cloud density for BIOL-L14. (a) Map view of surface density (in points/m^2) calculated within a 0.01 m radial distance of each point. Calculations performed on the un-interpolated point cloud. Outer perimeter of the microatoll is shown with a dashed red line. **(b)** Histogram of point cloud density for BIOL-L14.

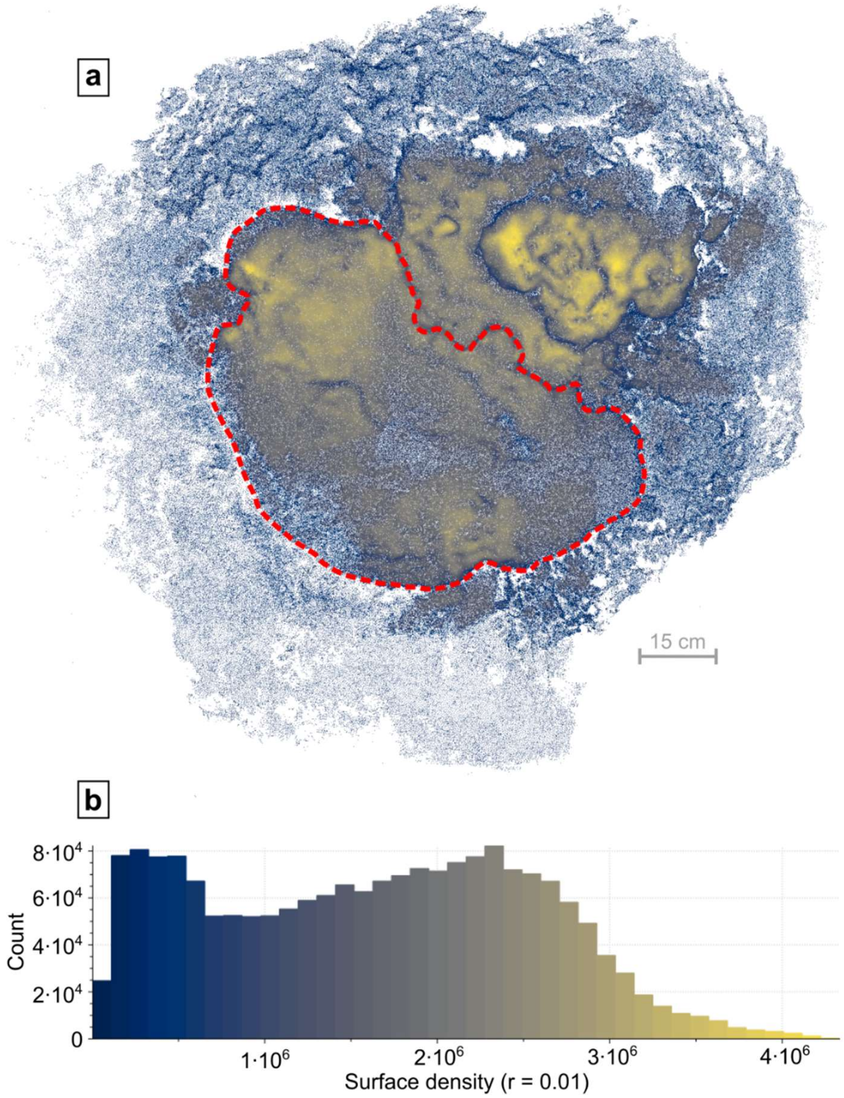

Figure S10. LiDAR point cloud density for BIOL-L3. (a) Map view of surface density (in points/m^2) calculated within a 0.01 m radial distance of each point. Calculations performed on the un-interpolated point cloud. Outer perimeter of the microatoll is shown with a dashed red line. **(b)** Histogram of point cloud density for BIOL-L3.

LiDAR point clouds were interpolated to 0.001 m resolution and exported as digital surface models (DSMs) using CloudCompare (Figures S11, S12, S13).

Unlike structure-from-motion photogrammetry, LiDAR scans are inherently scaled. Nonetheless, to check the accuracy of the internal scaling, we surveyed distinctive features on the surface of BIOL-L14 using a total station with a minimum accuracy of approximately 2 mm when surveying a target at a ~100 m distance (Trimble Inc., 2025). Distances between pairs of surveyed points and equivalent positions on the LiDAR model do not differ by more than 4 mm (Table S3). The average difference between pairs of surveyed points and equivalent positions on the LiDAR model is 1.9 mm.

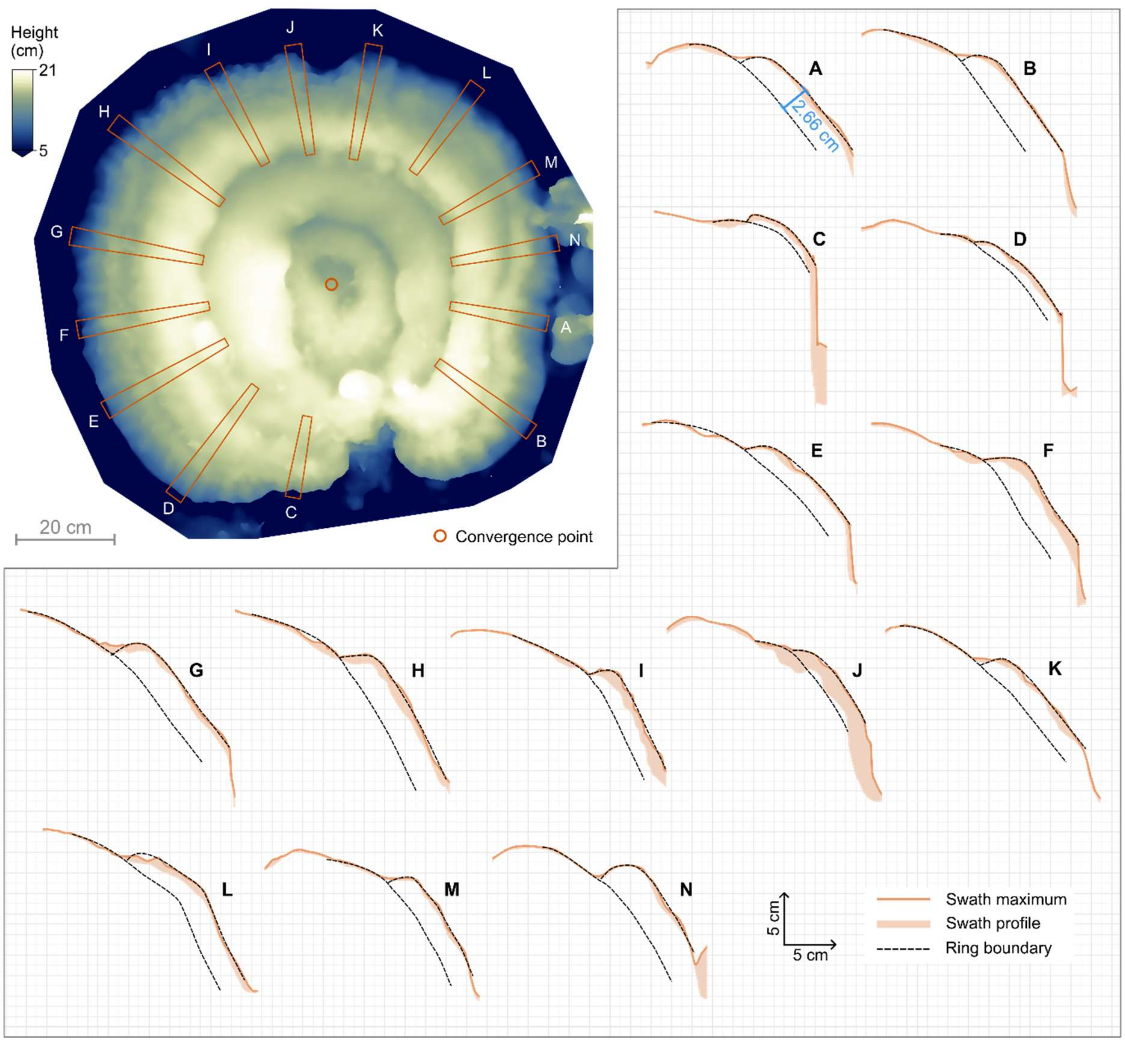

Figure S11. BIOL-L14's digital surface model, radial swath profiles and interpreted ring boundaries. Swath profiles are truncated to only cover the outer rings of the microatoll for ease of viewing. The convergence point of the swath profiles is the approximate centre of growth of the microatoll. Example of an outer ring thickness measurement is shown on profile 'A'. Height is elevation above the neighbouring reef substrate within the LiDAR scan area, and, while relative heights characterize the vertical extent of the microatoll, absolute height magnitude should be considered arbitrary.

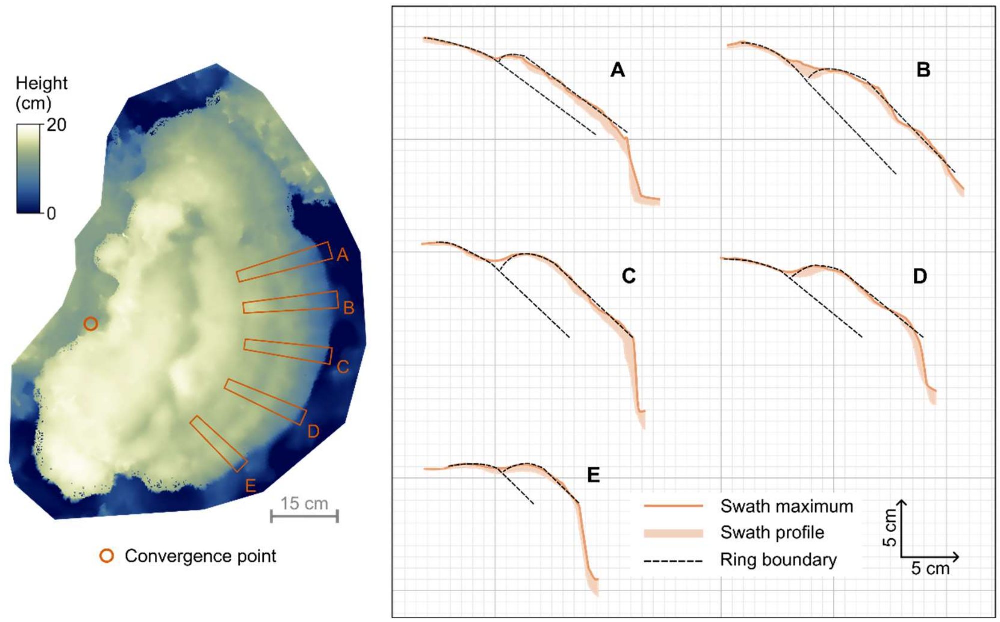

Figure S12. BIOL-L3's digital surface model, radial swath profiles and interpreted ring boundaries. The convergence point of the swath profiles is the approximate centre of growth of the microatoll. Height is elevation above the neighbouring reef substrate within the LiDAR scan area, and, while relative heights characterize the vertical extent of the microatoll, absolute height magnitude should be considered arbitrary.

To measure the thickness of the outer ring using the DSM, height swaths were produced from equally spaced radial profiles that subtend an angle of 4° from the microatoll's centre of growth to circumference (Figures S11, S12, S13). We then truncated the profiles to cover only the living outer rim and the outermost dead ring. Microatolls BIOL-L3 and BIOL-L13 do not have circular planform geometry so their initial growth positions may not lie in the geometric centre of the microatoll. Therefore, for BIOL-L3 and BIOL-L13, we drew five profiles perpendicular to the arc of the outer living rim (Figure S12, S13). On BIOL-L13, the outer ring appears to have grown over part of the crest of the adjacent inner ring (Figure S14). Therefore, we restrict our profiles to the area between A–E on Fig. S13 for this coral.

Ring boundaries were extrapolated from the maximum of each swath profile. All swath profiles and inferred ring boundaries are shown in Figures S11, S12 and S13. All ring thicknesses are provided in Supplementary Spreadsheet 1.

BIOL-L3's outer ring thickness measured from the digital surface model (Figure S12) is 3.15 ± 0.86 cm (1σ). The HLG of BIOL-L3 (measured in May 2023 using a total station) was 40.56 ± 2.15 cm above ACD (1σ; n = 4). Using a growth rate of 1.75 ± 0.5 (1σ) cm yr^{-1} to account for the three months of vertical growth during the period between the HLG survey and the LiDAR scan (in August 2023), we estimate the average HLS after BIOL-L3's most recent diedown prior to 2022 (the 'pre-2022 diedown HLS') to be 37.85 ± 2.32 cm above ACD (1σ). Exposure of BIOL-L3, relative to its pre-2022 diedown HLS, is shown in Fig. S16.

The 2023 HLG of BIOL-L13 was surveyed on 5th August 2023. BIOL-L13's 2023 HLG on 5th August 2023 was 50.87 ± 0.86 cm above ACD (1σ; n = 8). The average ring thickness measured from the digital surface model is 2.72 cm, with a standard deviation of 0.47 cm (Figure S13). Since the LiDAR scan and total station survey of HLG were conducted on the same day, no further correction for microatoll growth is necessary, and BIOL-L13's pre-2022 diedown HLS is 48.15 ± 0.98 cm above ACD (1σ). Exposure of BIOL-L13, relative to its pre-2022 diedown HLS, is shown in Fig. 6 of the main text.

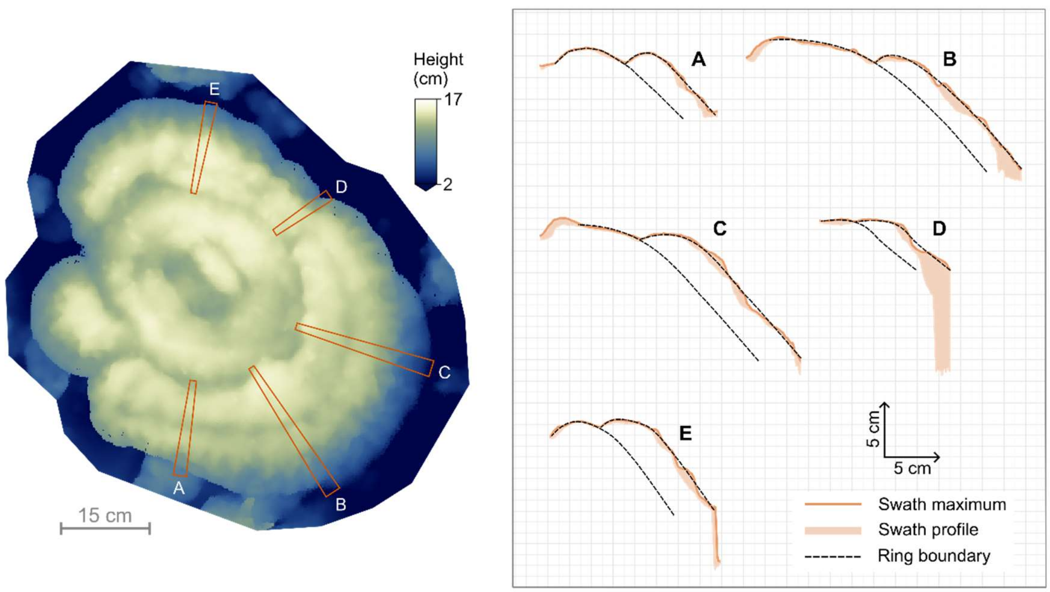

Figure S13. BIOL-L13's digital surface model, radial swath profiles and interpreted ring boundaries. Height is elevation above the neighbouring reef substrate within the LiDAR scan area, and, while relative heights characterize the vertical extent of the microatoll, absolute height magnitude is arbitrary.

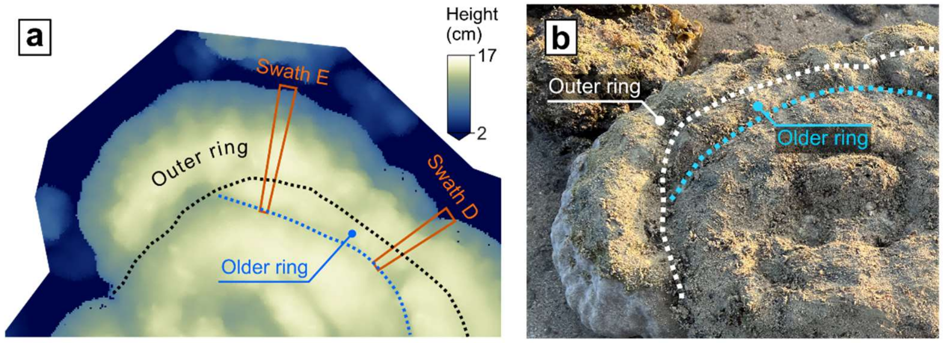

Figure S14. (a) Section of BIOL-L13's digital surface model shown in Fig. S10 with the inner boundary of the outer ring (black lines and labels) and the previously formed 'older ring' shown using dotted lines. (b) The same ring boundaries annotated on a photograph of BIOL-L13 from 5th August 2023. The blue dotted line in (a) corresponds to the blue dotted line in (b); the black dotted line in (a) corresponds to the white dotted line in (b).

Table S3. Vertical differences (ΔZ) between pairs of points—D1–D3, C(3), R3(4)—surveyed using a survey rod and total station, and the vertical differences measured from equivalent locations on BIOL-L14's digital surface model. All values in metres. TS: Total station. DSM: Digital surface model.

ΔZ (TS survey)

	D1	**D2**	**D3**	**C(3)**	**R3(4)**
D1		0.003	0.035	0.059	0.049
D2			0.032	0.056	0.046
D3				0.024	0.014
C(3)					-0.01
R3(4)					

ΔZ (DSM)

	D1	**D2**	**D3**	**C(3)**	**R3(4)**
D1		0.005	0.034	0.061	0.052
D2			0.029	0.056	0.047
D3				0.027	0.018
C(3)					-0.01
R3(4)					

ΔZ (TS survey) − ΔZ (DSM)

	D1	**D2**	**D3**	**C(3)**	**R3(4)**
D1		0.002	0.001	0.002	0.003
D2			0.003	0.000	0.001
D3				0.003	0.004
C(3)					0.000
R3(4)					

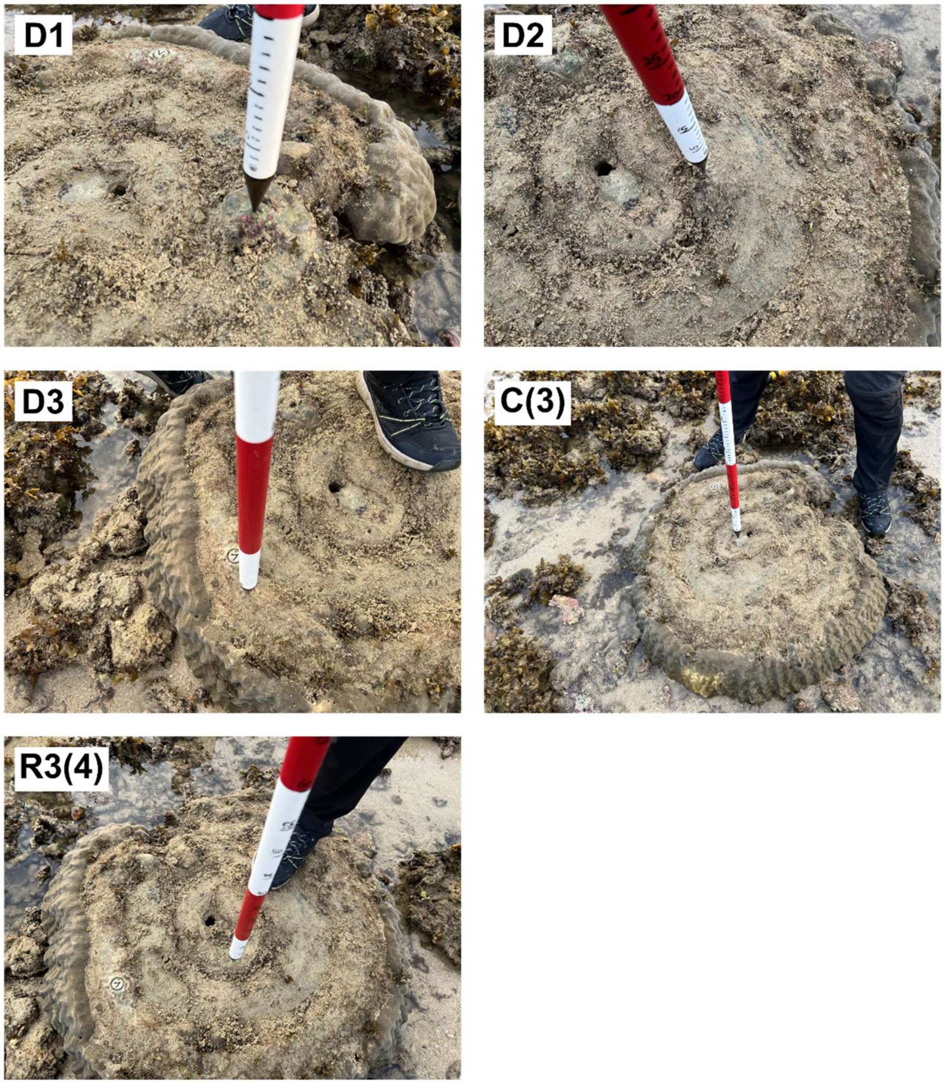

Figure S15. Photographs showing the points in Table S3 being surveyed using a survey rod.

5. Subaerial exposure of BIOL-L3 in 2021

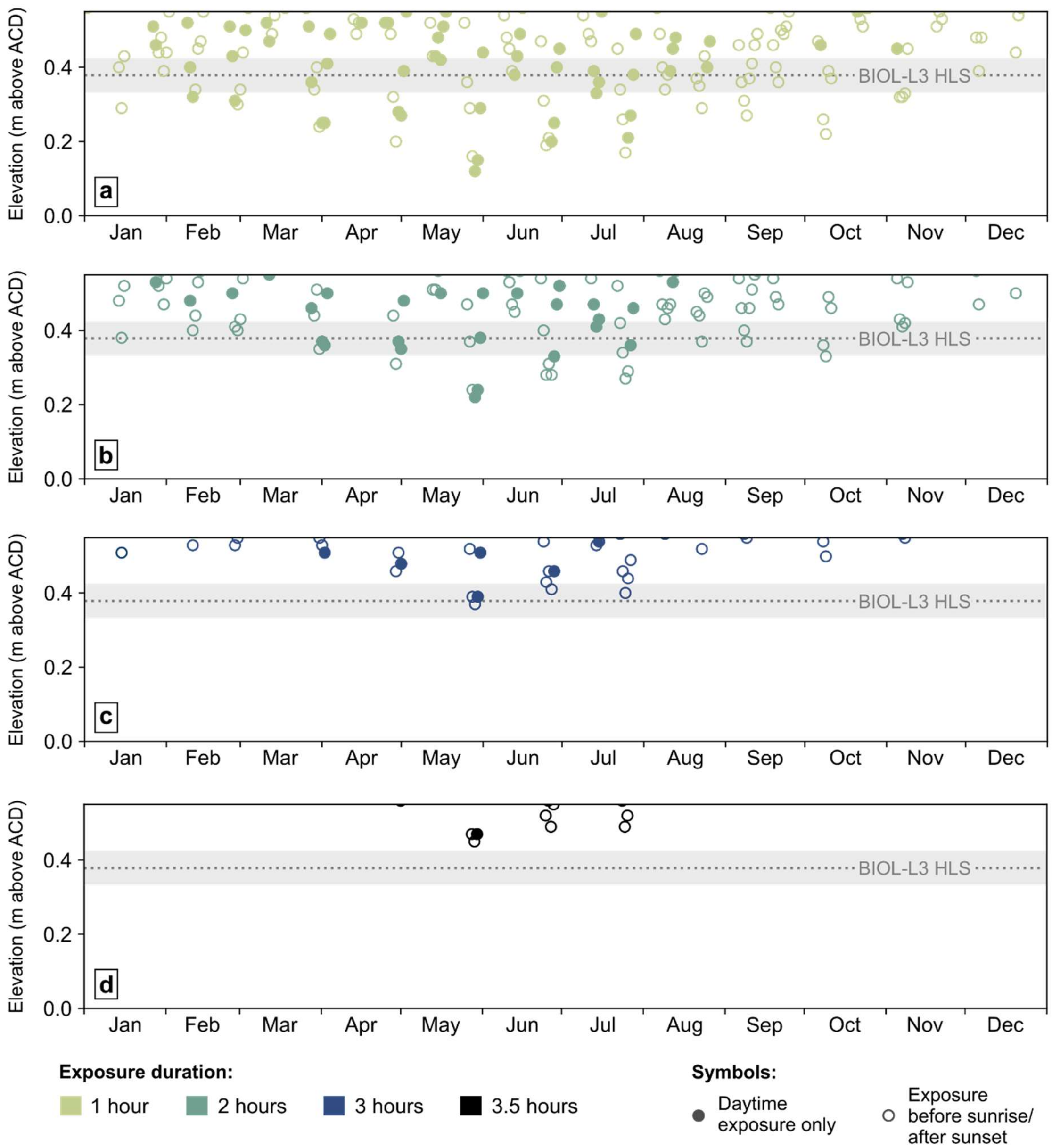

Figure S16. Lowest elevation exposed for a one-, two-, three- or 3.5-hour interval each day during 2021, based upon the Raffles Lighthouse tide-gauge data, and the elevation of HLS on BIOL-L3. Filled circles denote low tides that occurred entirely between sunrise and sunset, while hollow circles represent exposure that occurred partially or wholly before sunrise or after sunset. HLS: Mean (dotted line) and two standard deviations (shaded area) of the highest level of survival for the most recent diedown prior to BIOL-L3's first observation in June 2022. HLS was estimated using ring thickness measured from the digital surface model (Figure S12) and a field survey of the living outer rim in 2023.

BIOL-L3 would have been exposed to an elevation significantly lower than its pre-2022 diedown HLS for two consecutive hours on nine occasions in 2021 (Figure S16b), but this microatoll was not exposed to an elevation significantly lower than the pre-2022 diedown HLS for three or more consecutive hours in 2021 (Figure S16c). BIOL-L3 was partially exposed down to the elevation of its pre-2022 diedown HLS, within error, for three consecutive hours in May, June and July 2021 (Figure S16c).

6. Elevations of the Siloso Point microatolls

Table S4. Surveyed highest level of growth (HLG) and the extrapolated HLG to 29th May 2021 for the Siloso Point microatolls. All elevations are in metres and are relative to SHD.

Coral ID	Survey date	Minimum surveyed HLG	Maximum surveyed HLG	Minimum extrapolated HLG[1]	Maximum extrapolated HLG[2]
SILO-L1	1st May 2021	-1.364	-1.328	-1.364	-1.326
SILO-L2	24th July 2020	-1.345	-1.308	-1.341	-1.283
SILO-L4	1st April 2021	-1.415	-1.385	-1.414	-1.380
SILO-L5	29th May 2021	-1.481	-1.391	-1.481	-1.391

[1]Minimum extrapolated HLG calculated using minimum surveyed HLG, the number of days between the survey date and 29th May 2021 and a growth rate of 0.5 cm yr^{-1} for SILO-L1, -L2 and -L4 (all surveyed before 29th May 2021) / a growth rate of 3 cm yr^{-1} for SILO-L5 (surveyed after 29th May 2021).

[2]Maximum extrapolated HLG calculated using the maximum surveyed HLG, the number of days between the survey date and 29th May 2021 and a growth rate of 3 cm yr^{-1} for SILO-L1, -L2 and -L4 / a growth rate of 0.5 cm yr^{-1} for SILO-L5.

References

Luetzenburg, G., Kroon, A. and Bjørk, A.A., 2021. Evaluation of the Apple iPhone 12 Pro LiDAR for an application in geosciences. *Scientific reports*, *11*(1), pp.1-9.

Luetzenburg, G., Kroon, A., Kjeldsen, K.K., Splinter, K.D. and Bjørk, A.A., 2024. High-resolution topographic surveying and change detection with the iPhone LiDAR. *Nature Protocols*, pp.1-22.

Tan, F., Horton, B.P., Ke, L., Li, T., Quye-Sawyer, J., Lim, J.T., Peng, D., Aw, Z., Wee, S.J., Yeo, J.Y., Haigh, I., Wang, X., Aung, L.T., Mitchell, A., Sarkawi, G., Li, X., Tan, N.S. and Meltzner, A.J., 2024. Late Holocene relative sea-level records from coral microatolls in Singapore. *Scientific Reports*, *14*(1), p.13458.

Tan, N.S., Gautam, R. Tan, F. Sarkawi, G.M., Majewski, J.M., Komori, J. Wee, S.J., Leoh, K.K., Koh, L.D., Switzer, A.D., Meltzner, A.J., 2025. Three-dimensional models of coral microatolls using structure-from-motion photogrammetry and iPhone LiDAR scanning: A fast, reproducible method for collecting relative sea-level data in the field. *Under review*

Trimble Inc., 2025 https://geospatial.trimble.com/en/products/hardware/trimble-c5 [Accessed: May 2025]